Supporting Information

Bioinspired Design of Ca^{2+} Induced Artificial Signal Transduction Systems: ON/OFF Emitting Bacteria and Excimer-FRET Signalling-Induced Bactericidal Activity

Subrata Das, Raki Mandal, Rahul Prakash, Sandini P., Sampurna Roy and Pradip Kumar Tarafdar*

Department of Chemical Sciences, Indian Institute of Science Education and Research Kolkata, Mohanpur 741246, West Bengal, India

Email: tarafdar@iiserkol.ac.in

Contents:

1. General information

All the reactions have been performed under an inert atmosphere (Ar or N_2) in oven-dried glassware, unless specified otherwise. Reaction temperatures correspond to the temperature of the bath surrounding the vessel.

Synthesis related analytics: ^1H, and ^{13}C-NMR spectra have been recorded on Bruker Avance (^1H: 500 MHz, ^{13}C {^1H}: 126 MHz) and JEOL (^1H: 400 MHz, ^{13}C {^1H}: 101 MHz) NMR spectrometer at room temperature (~23 °C) and are referenced to the resonances of the solvent used. The NMR spectra were analysed using MestReNova software. Multiplicities have been indicated as, s (singlet), d (doublet), t (triplet), dd (doublet of doublet), dt (doublet of triplet) or m (multiplet). Coupling constants (*J*) are reported in Hertz (Hz). Mass spectra were recorded using a Bruker micrOTOF-Q II or a Waters QTOF Spectrometer. Flash chromatography was carried out on an automated system (Combiflash NEXTGEN 300+) using pre-packed cartridges of silica (50 µm Redisep®Rf Teledyne Isko Column). For thin-layer chromatography (TLC) analysis, Merck pre-coated TLC plates (silica gel 60 F254 0.25 mm) were used, and visualisation was accomplished by UV light (254 nm), I_2, $KMnO_4$, cerium ammonium molybdate, H_2SO_4, and ninhydrin.

Chemicals: Commercially available chemicals were purchased from Sigma–Aldrich (Merck), Alfa-Aesar, Avra Synthesis, and BLD Pharma and used without further purification. Lipids were acquired from Avanti Polar Lipids Inc. Dry solvents were prepared according to the standard procedure and before use. Lithocholic acid and 1-Pyrenebutyric acid were bought from Sigma-Aldrich (Merck). Boc-L-Histidine, L-aspartic acid, N, N'-dicyclohexylcarbodiimide (DCC), hexafluorophosphate azabenzotriazole tetramethyl uronium (HATU), 4-dimethylaminopyridine (DMAP), N-(3-Dimethylaminopropyl)-N’-ethyl carbodiimide hydrochloride (EDC.HCl), di-*tert*-butyl dicarbonate (Boc anhydride), rhodamine B (RhB), calcium chloride dihydrate, magnesium chloride hexahydrate, sodium chloride, potassium chloride, ethylenediaminetetraacetic acid (EDTA), and TRIS buffer were bought from Sisco Research Laboratory, India. HCl, NaOH, Na_2SO_4, NaCl, and other salts were bought from

Merck. All the chemicals were used without further purification. The buffer was prepared using Milli-Q water.

2. Preparation of vesicles:

The model membranes (vesicles) were prepared using DOPC and DOPE at a ratio of 60:40 by following the standard protocol in the literature.[1] A thin film of DOPC and DOPE (maintaining a molar ratio of 60:40) was prepared in a glass vial via the evaporation of the chloroform solution using a nitrogen purge. The glass vial with lipid film was dried overnight to remove the residual organic solvent under vacuum. The film was hydrated with a 10 mM pH 8 TRIS buffer and the overall lipid concentration was maintained at 4 mM. The mixture was vortexed vigorously for 2 hours. The large unilamellar vesicles (LUVs) were prepared by extruding the lipid suspension through 100 nm polycarbonate filters 19 times. The size of the vesicles was measured on Malvern Zetasizer Nano ZS, UK. The average size of the vesicles was ~ 110 nm.

3. Dynamic light scattering (DLS):

The size of vesicles and transducer self-assembly was measured using a Malvern Zetasizer Nano ZS (Malvern Instruments Ltd., UK) equipped with a He-Ne laser (wavelength: 633 nm). The size of the vesicles remains unchanged after the addition of transducers. Experiments were performed at least three times, and the average with standard deviation was plotted.

4. Isothermal Titration Calorimetry (ITC):

ITC studies were carried out using a MicroCal PEAQ-ITC instrument (Malvern) to investigate the binding interaction of PyLAD with calcium ions. 0.2 mM PyLAD was taken in the cell and titrated with 3 mM Ca^{2+} in tris buffer (10 mM, pH 8) taken in the syringe at 25 °C. The ITC isotherms were fitted to a 'one set of sites' model to determine the thermodynamic parameters and stoichiometry (N).

5. Nile Red assay for critical aggregation concentration (CAC) determination:

Nile Red (NR) assay is one of the convenient methods to calculate critical aggregation concentration (CAC). 1 µM NR was added (stock solution in acetone) to the 10 mM tris buffer, pH 7.4. The solution was excited at 530 nm, and the emission was recorded from 550-700 nm. Transducers (PyLAD, PyLAA, PyLAE) were added from a stock solution, equilibrated and the fluorescence emission spectra were recorded. The emission intensity at 635 nm was plotted against the concentration of transducers. The concentration at which the NR fluorescence intensity starts increasing, was evaluated to determine the CAC.

6. Fluorescence spectroscopy and signal transduction:

Fluorescence measurements were performed using an F-7000 HITACHI spectrofluorometer equipped with a quartz cuvette. Vesicle suspensions composed of DOPC: DOPE (3:2 molar ratio; 0.4 mM lipid concentration, ~100 nm diameter) were prepared in 10 mM Tris buffer (pH 8.0) and incubated with 10 µM of the respective transducer molecules (PyLAD, PyLAA, PyLAD^{t}Bu, and PyLAE). The samples were transferred to the cuvette, and fluorescence emission spectra were recorded upon excitation at 334 nm, with emission recorded from 350 to 550 nm. The monomeric pyrene emission at 382 nm (I_3) was used for normalization, enabling quantitative comparison of the excimer emission intensity at 472 nm upon the stepwise addition of calcium ions or other metal ions as the input signal. Normalized emission spectra were plotted to evaluate the signal-transducing efficiencies of the transducers.

7. Preparation of giant unilamellar vesicles (GUVs) and Fluorescence Lifetime Imaging Microscopy (FLIM):

GUVs were prepared using a reported literature.[2] DOPC/DOPE (60: 40) was dissolved in 1 mL of $CHCl_3$-methanol (3:1) and placed in an RB flask. Next, 4 ml of buffer (pH 8, 10 mM TRIS buffer) was added, and the concentration of lipids was 2 mM. The solution was then rotated at 40 ^{o}C under reduced pressure to completely evaporate the organic component. GUV formation was characterised under an optical microscope. 10 µM PyLAD was added to the 0.4 µM GUVs solution and incubated for 10 minutes. A confocal laser scanning inverted microscope (Axio Observer A1) from Zeiss, coupled to a DCS-120 system from Becker and Hickl GmbH (BH), was used to record FLIM images. The excitation source was a picosecond diode laser (λ_{ex} = 405 nm; BDL-488-SMC; BH). A BH GVD-120 controller was used to control the scanning. The BH HPM-100-40 hybrid detector module in the DCS-120 system was controlled with DCC-100 software.

8. Transmission Electron Microscopy (TEM):

Samples were prepared following the previous literature report[3] with necessary modifications. Briefly, a tiny amount of the aqueous solution (30 µM overall concentration) of the aggregates (PyLAD) was drop-cast and allowed to adsorb on the 300 square mesh Cu grid manufactured by TED PELLA, INC. The excess aqueous solution was soaked in filter paper. The grid was then stained with uranyl acetate and dried overnight in a vacuum, and the images were subsequently recorded in JEOL JEM-2100F microscopes.

9. Bacterial growth:

The Luria-Bertani (LB) broth was prepared using Milli-Q water and sterilised by autoclaving at 120 °C for 120 minutes. *Escherichia coli* cells were grown in LB medium at 37 °C with shaking (180-200 rpm) until the OD_{610} reached ~ 1.0-1.2. Cells were harvested by centrifugation at 4000 × g for 5 min and washed twice with phosphate-buffered saline (PBS, pH 7.4). The bacteria were resuspended in PBS (pH 7.4) to prepare bacteria stock. 10 mM solutions of the synthetic transducers (PyLAD and PyLAE) were prepared in HPLC-grade dimethyl sulfoxide. 5 mL of LB media and a bacterial aliquot (~200-fold dilution of bacterial stock) were taken in autoclaved test tubes. Transducers and 5 mM Ca^{2+} were added immediately to the appropriate test tubes. The control and the test tubes containing bacteria were incubated at 37 °C for 10-12 hours. Optical density at 610 nm was measured using an Epoch 2 Microplate Spectrophotometer (BioTek) to monitor time-dependent bacterial growth. All the experiments were performed in triplicate.

10. Confocal microscopy:

Confocal laser scanning microscopy (CLSM) was performed using a Leica SP8 system (Leica Microsystems, Wetzlar, Germany) equipped with an HC PL APO 63x/1.40 oil immersion objective. *Escherichia coli* cells were grown in Luria-Bertani medium at 37 °C with shaking (180-200 rpm) until mid-log phase (OD_{610} ≈ 0.4-0.6). Cells were harvested by centrifugation at 4000 × g for 5 min and washed twice with phosphate-buffered saline (PBS, pH 7.4). The bacteria were resuspended in PBS, pH 7.4. 10 µM PyLAD was incubated with *E. coli*. A small volume (8-10 µL) of the bacterial suspension was placed onto the glass surface, covered with a cover slip and allowed to settle for 5-10 min. Confocal experiments were performed using a 405 nm laser with *E. coli*. Next, 5 mM Ca^{2+} was added, and the confocal images were acquired. Subsequently, 5 mM EDTA was added, and the images were captured. In another set of experiments, 10 µM PyLAD or PyLAE and 2.5 µM RhB were incubated with *E. coli*. Confocal experiments of the sample, sample 1 (sample + 5 mM Ca^{2+}) and sample 2 (sample + 5 mM Ca^{2+} + 5 mM EDTA) were performed using a 405 nm laser.

11. STED (Stimulated emission depletion) microscopy:

An Abberior Facility Line system with an Olympus IX83 microscope (Abberior Instruments) was used for STED imaging. The Abberior autoalignment sample was utilized to align the STED and confocal channels. A 30 nm pixel size was maintained during imaging. A pulsed STED line

at 775 nm was used for depletion. A 1.0-1.5% (w/v) agar-agar solution was prepared by dissolving agar in Milli-Q water. The solution was heated to boiling with continuous stirring until complete dissolution and then maintained at ~50-55 °C to prevent premature solidification. Approximately 50-100 µL of molten agar solution was added to each well of a glass-bottom confocal plate and gently spread to form a thin, uniform agar layer (~100-200 µm) covering the glass surface. Excess agar was avoided to minimize optical aberrations during high-NA imaging. The plate was allowed to cool and solidify at room temperature for 5-10 min under sterile conditions, forming a smooth and optically homogeneous surface. *E. coli* cultures were grown to mid-log phase (OD_{600} ≈ 0.4-0.6) at 37 °C with shaking. Then, bacteria were harvested by gentle centrifugation (3000-4000 × g, 5 min) and resuspended in PBS 1X (pH 7.4). *E. coli* was incubated with 1 µM Nile Red and 10 µM PyLAD for imaging in PBS (pH 7.4). A small aliquot (10-20 µL) of the labelled *E. coli* suspension was gently pipetted onto the solidified agar layer. Bacteria cells were allowed to settle and partially embed into the agar surface for 5-10 min at room temperature. The confocal plate was sealed with cover slip to prevent evaporation and directly mounted on the STED microscope stage. The signal transducer PyLAD was imaged in the confocal channel, while Nile Red (NR) was detected in the STED channel. Following the addition of 5 mM Ca^{2+}, a pronounced cyan emission arising from signal transduction was observed upon 405 nm excitation. This emission showed colocalization with the bacterial membrane marker NR (excited at 568 nm) (**Figure S20**).

12. Excimer-FRET signalling and bacterial growth under photoirradiation:

10 µM transducers (PyLAD or PyLAE) and 1.5-2.5 µM RhB were dissolved in 5 mL of oxygenated LB media and placed in autoclaved test tubes. A bacterial aliquot (~200-fold dilution of the bacterial stock) and 5 mM Ca^{2+} were added to the appropriate test tubes. Next, the test tubes were photoirradiated with a 370 nm Kessil lamp (75% power, 40 W) for 10 minutes, followed by incubation at 37 °C for 10 hours. Control experiments were performed under no photoirradiation. Optical density at 610 nm was measured using an Epoch 2 Microplate Spectrophotometer (BioTek) to monitor time-dependent bacterial growth. All the experiments were performed in triplicate.

13. Synthetic scheme for the transducer molecules:

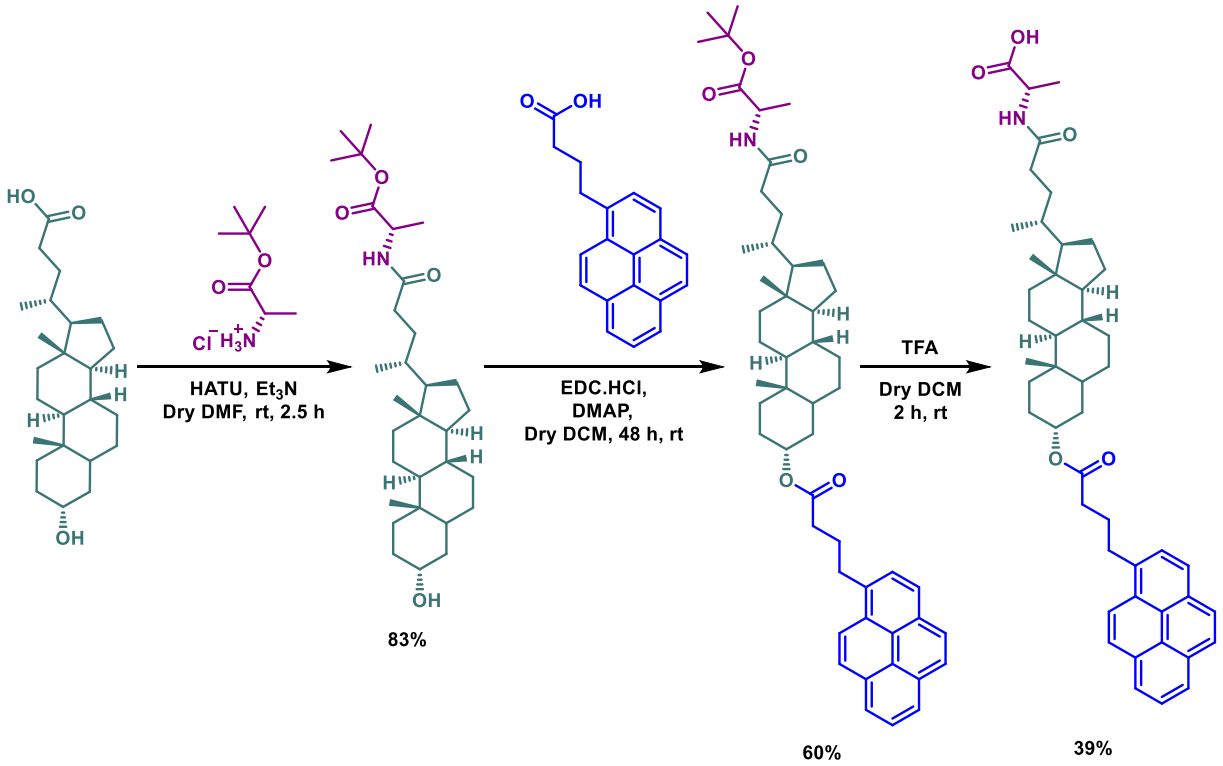

***Scheme S1**: Synthetic scheme of PyLAA.*

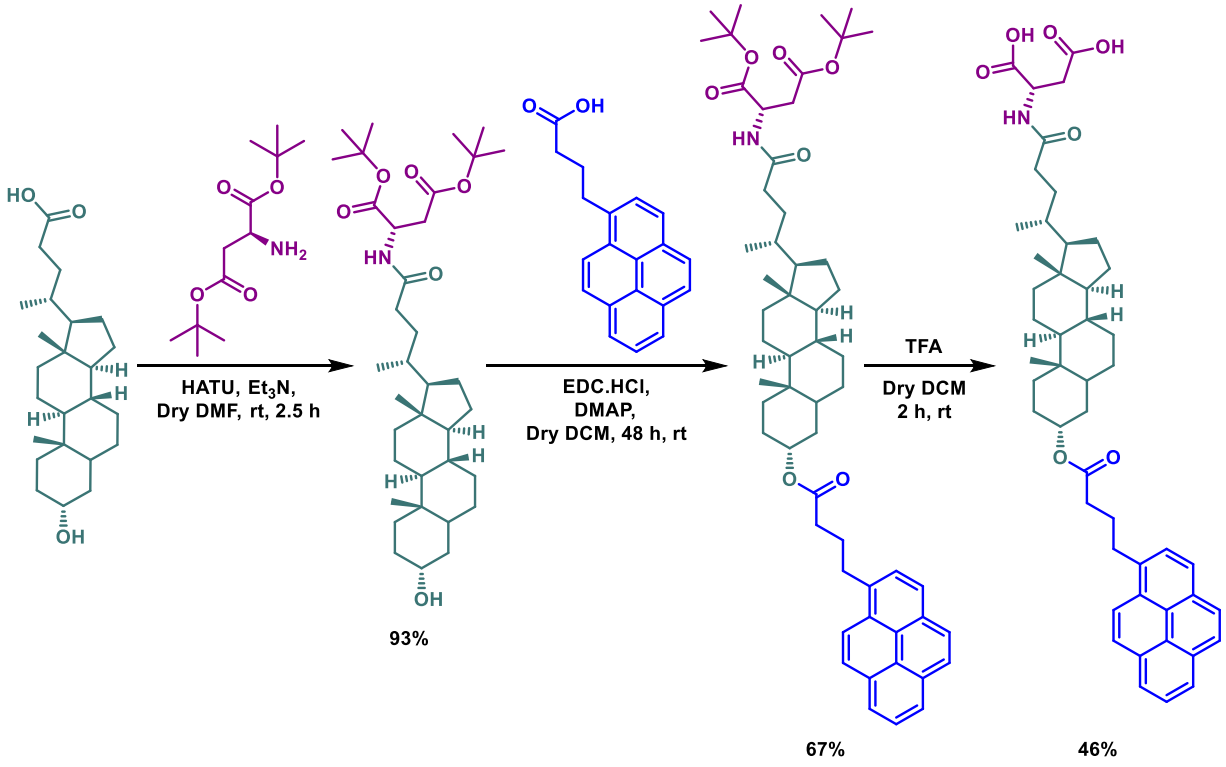

***Scheme S2**: Synthetic scheme of PyLAD.*

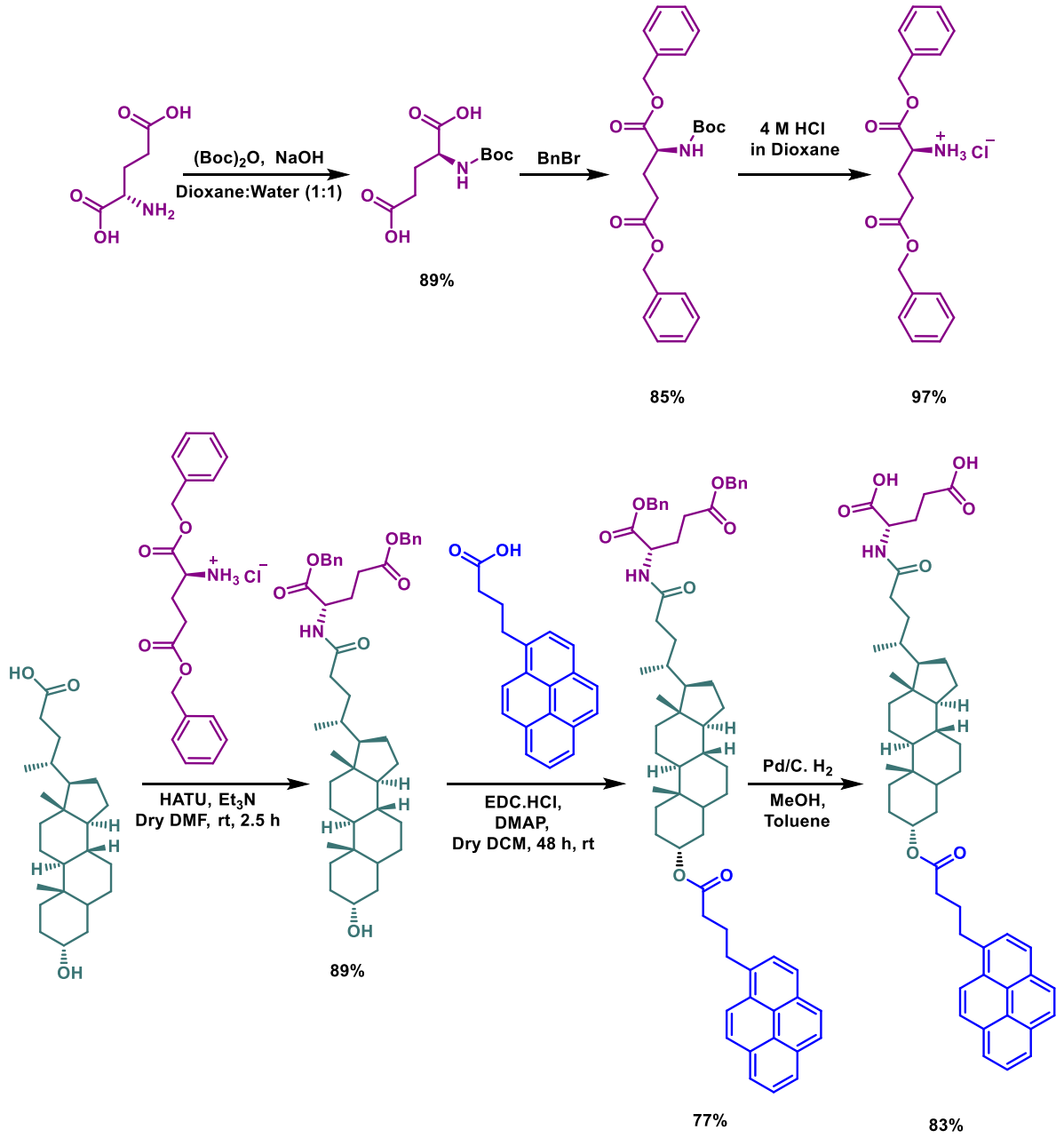

***Scheme S3**: Synthetic scheme of PyLAE.*

14. General procedure for synthesis of transducers:

14.1. General procedure for Boc-protection of amino acid (GP1):

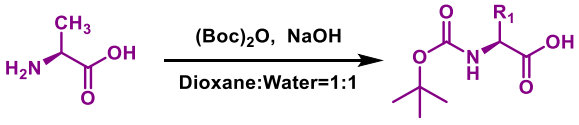

A solution of L-amino acid (1.0 equiv.) in a mixture of dioxane (10 mL), water (10 mL), and 1N NaOH (10 mL) was stirred and cooled in an ice-water bath to 0 °C. Di-tert-butyldicarbonate (1.2 equiv.) was added, and stirring was continued at room temperature for the next 6 hours. Then, the solution was concentrated under vacuum, cooled in an ice-water bath, dissolved in

50 mL ethyl acetate, and acidified with a dilute solution of $KHSO_4$ until the pH reached ~2–3. The aqueous phase was extracted with ethyl acetate. followed by drying of the combined organics over anhydrous Na_2SO_4 and evaporation under reduced pressure to obtain the product.

14.2. General procedure for benzyl-protection of amino acid (GP2):

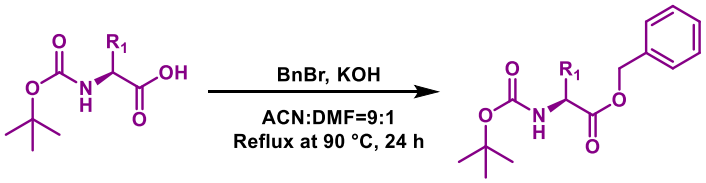

The Boc-protected compound (1 equiv.) obtained via **GP1** was dissolved in 10 mL of dry acetonitrile (ACN) and dry dimethylformamide (DMF) in a 9:1 ratio in a round-bottom flask. Then, KOH (1.1 equiv.) and benzyl bromide (1.1 equiv.) were added to the flask followed by subjecting the reaction mixture to reflux at 90 ^oC for 24 hours under nitrogen atmosphere. The reaction was monitored via thin layer chromatography (TLC). ACN and DMF were evaporated, and the residue was dissolved in cold water followed by extraction with ethyl acetate (60 mL). The organic layer was dried over anhydrous sodium sulphate and evaporated under vacuum to yield the crude reaction mixture. The product was purified in silica gel (230-400 mesh) using ethyl acetate in hexane solvent mixture as eluent under flash column chromatography.

14.3. General procedure for the synthesis of t-butyl ester of amino acid (GP3):

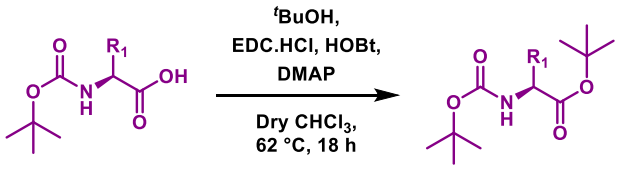

The Boc-protected amino acid (1 equiv.) synthesized via **GP1** was added to a round-bottom flask, followed by 1-hydroxybenzotriazole (HOBt) (1.5 equiv.) and N-(3-dimethylaminopropyl)-N'-ethylcarbodiimide hydrochloride (EDC.HCl) (1.5 equiv.) along with 30 mL of anhydrous $CHCl_3$ under argon atmosphere, and the resultant reaction mixture was allowed to stir for 30 min. Next, 4-(dimethylamino)pyridine (DMAP) (4 equiv.) was added, and ^{t}butanol (1.1 equiv.) was injected via syringe. Then, the reaction mixture was subjected to reflux at 62 ^oC for 18 hours under argon atmosphere. The reaction progress was monitored via TLC. After the completion of the reaction, the solvent was evaporated to dryness, and the residue was dissolved in diethyl ether (30 mL). The organic layer was washed with 10% w/v

sodium bicarbonate solution (2*10 mL), 10% w/v citric acid solution (2*10 mL), 10% w/v potassium carbonate solution (2*10 mL) and brine (2*10 mL). Then the combined organics were dried over anhydrous sodium sulphate, and the solvent was removed under reduced pressure. The crude was purified by flash chromatography on silica gel to afford the pure product.

14.4. General procedure for Boc-deprotection of amino acid (GP4):

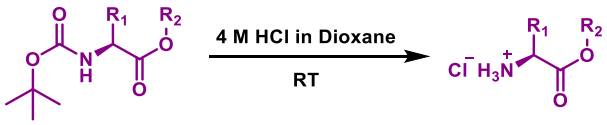

To the Boc-protected compound (2.0 mmol), 5 mL of HCl in dioxane (4 M) was added, and the removal of the Boc-group was monitored by thin-layer chromatography (TLC). After 6 hours, the solvent was removed under vacuum to get the desired product.

14.5. General procedure for the formation of an amide bond (GP5):

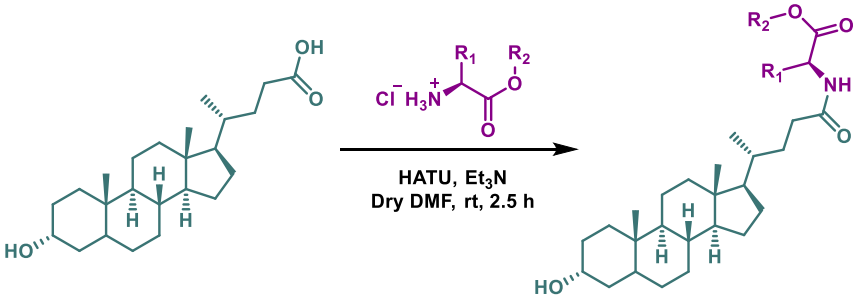

Lithocholic acid (1 equiv.) was dissolved in DMF (10 mL) followed by the addition of HATU (1.2 equiv.) and stirring of the reaction mixture for 15 minutes. Corresponding ^{t}butyl ester or benzyl-protected amino acid (1.2 equiv.) was added, followed by TEA (2.5 equiv.), and the reaction mixture was stirred for another 2.5 hours. The reaction was monitored via TLC. After the reaction was completed, the mixture was washed with water and extracted with EtOAc to yield a crude solid, which was then purified by column chromatography (Silica gel, mesh size 230-400) to obtain the pure compound.

14.6. General procedure for the formation of ester bond (GP6):

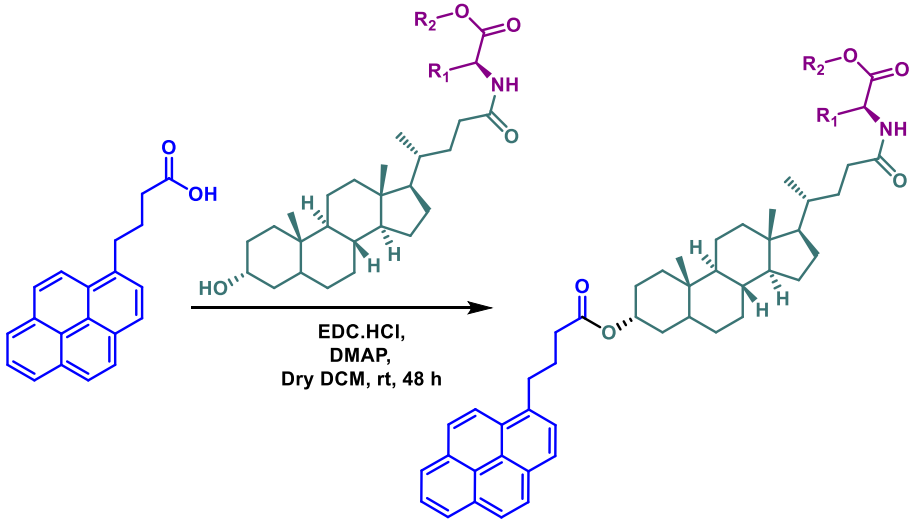

1-pyrenebutyric acid (1 equiv.). amide bonded lithocholic acid with the free hydroxyl group (1.2 equiv.), N-(3-Dimethylaminopropyl)-N′-ethyl carbodiimide hydrochloride (EDC.HCl) (1.2 equiv.) and DMAP (0.2 equiv.) were weighed out in a dried round-bottom flask and dissolved in dry DCM under N_2 gas at room temperature. The reaction mixture was then stirred for 48 hours and was monitored via TLC. After the completion of the reaction, an acidic workup using $KHSO_4$ and a basic workup using $NaHCO_3$ were performed, and the resulting mixture was collected in DCM (3 × 30 mL). The organic layer was dried over anhydrous Na_2SO_4 and concentrated under reduced pressure. The product was purified using column chromatography.

14.7. General procedure for the deprotection of t-butyl ester (GP7):

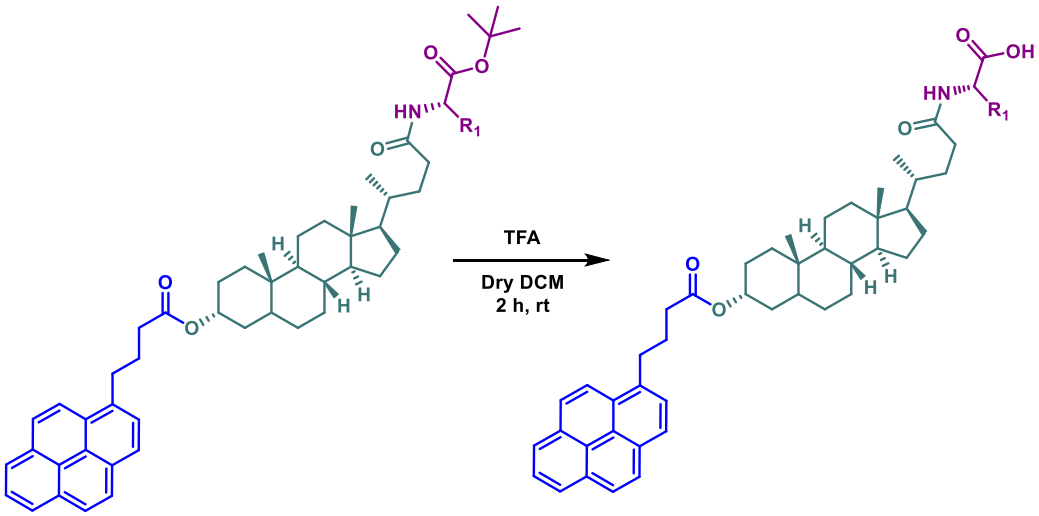

^{t}Butyl ester containing compound (1 equiv.) was taken in a dried round-bottom flask, dissolved in dry DCM and kept under N_2 gas at room temperature. After 5 minutes of stirring,

2 mL TFA was added dropwise to the reaction flask. This reaction system was stirred for the next 2 hours and monitored via TLC. After the reaction was completed, TFA was evaporated by diluting the reaction mixture three-fold with DCM. The compound was collected as a yellowish semi-solid.

14.8. General procedure for the benzyl-deprotection of amino acid (GP8):

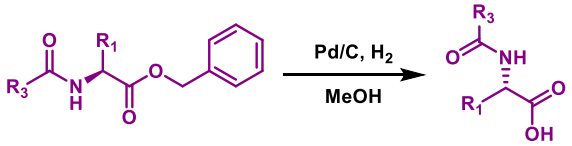

Benzyl ester containing compound (1equiv., 0.3 mmol) was taken in a dried round-bottom flask with 5 mL MeOH under N_2 gas at room temperature. After 5 minutes of stirring, a pinch of 10% Pd/C was added to the reaction flask. The reaction system was thoroughly purged with N_2 gas and stirred for the next 2 hours under an H_2 atmosphere (using a H_2 balloon) and was monitored via TLC. After the reaction was completed, the Pd/C catalyst was separated by filtering through a Celite bed in a sintered crucible and washed three times with methanol. The compound was collected as a yellowish semi-solid.

15. Synthetic procedure of transducers and their characterization:

15.1. Procedure for synthesis of PyLAA:

Transducer PyLAA was synthesized by following **GP1** (Yield: 98%), **GP3** (Yield: 85%), **GP4** (93%), **GP5** (Yield: 83%), **GP6** (Yield: 60%), **GP7** (Yield: 39%) sequence. **^{1}H NMR (400 MHz, $CDCl_3$)** δ 8.31 (d, J = 9.2 Hz, 1H), 8.17 – 8.09 (m, 4H), 8.04 – 7.95 (m, 3H), 7.86 (d, J = 7.8 Hz, 1H), 6.22 (d, J = 6.9 Hz, 1H), 4.88 – 4.67 (m, 1H), 4.67 – 4.48 (m, 1H), 3.38 (t, 2H), 2.45 (t, J = 7.2 Hz, 2H), 2.34 – 2.13 (m, 4H), 1.96 – 1.65 (m, 9H), 1.59 – 1.51 (m, 3H), 1.47 (d, J = 7.1 Hz, 3H), 1.39 – 1.34 (m, 4H), 1.26 – 1.20 (m, 3H), 1.12 – 0.96 (m, 7H), 0.92 – 0.88 (m, 6H), 0.62 (s, 3H). **^{13}C NMR (101 MHz, $CDCl_3$)** δ 175.6, 174.9, 173.3, 135.9, 131.5, 131.0, 130.1, 128.8, 127.6, 127.5, 127.5, 126.8, 125.9, 125.2, 125.1, 125.0, 124.9, 124.8, 123.5, 77.4, 77.1, 76.8, 74.6, 56.5, 56.0, 48.4, 42.8, 42.0, 40.5, 40.2, 35.8, 35.5, 35.1, 34.7, 34.5, 33.4, 32.9, 32.4, 31.7, 28.3, 27.1, 26.8, 26.4, 24.2, 23.4, 20.9, 18.4, 18.1, 12.1. **ESI-MS:** m/z 716.4311 $[M-H]^-$; Mcalcd: 716.4320.

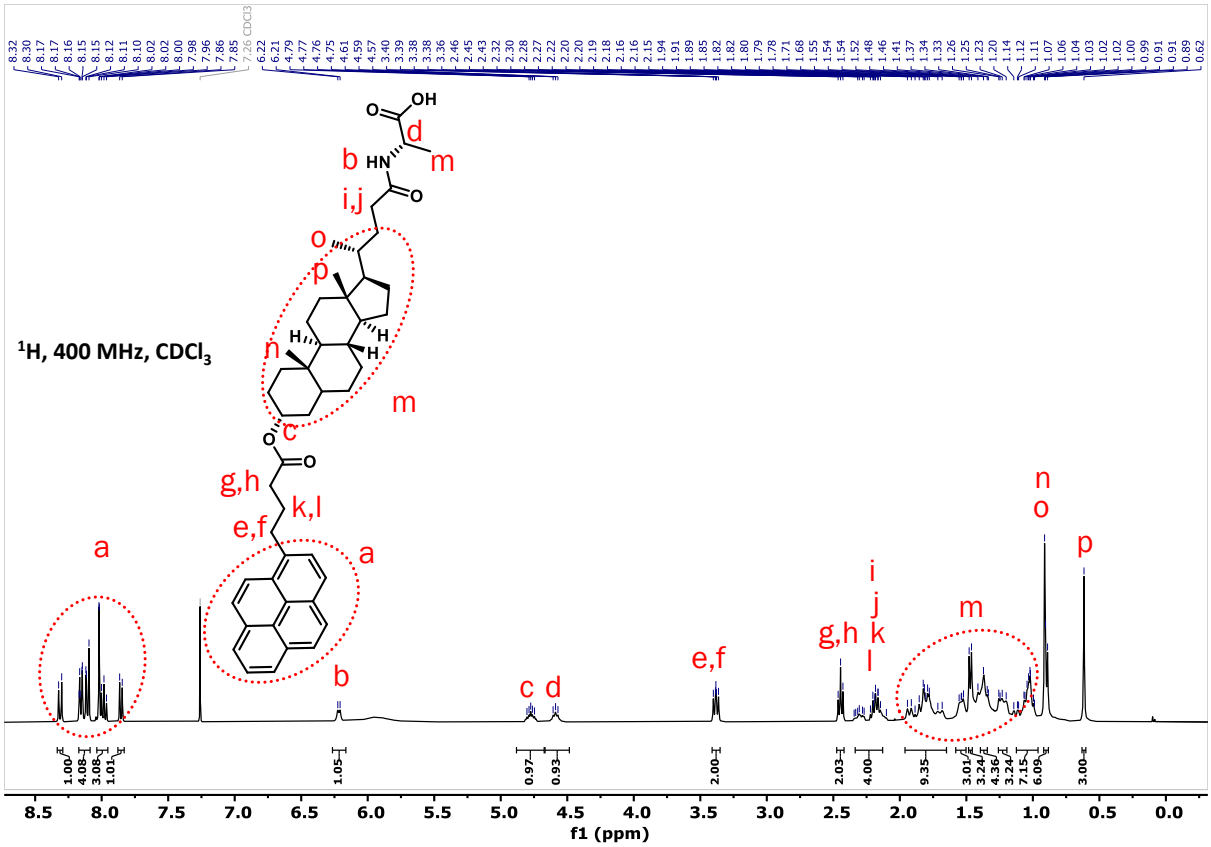

Figure S1: *^{1}H-NMR spectrum of PyLAA.*

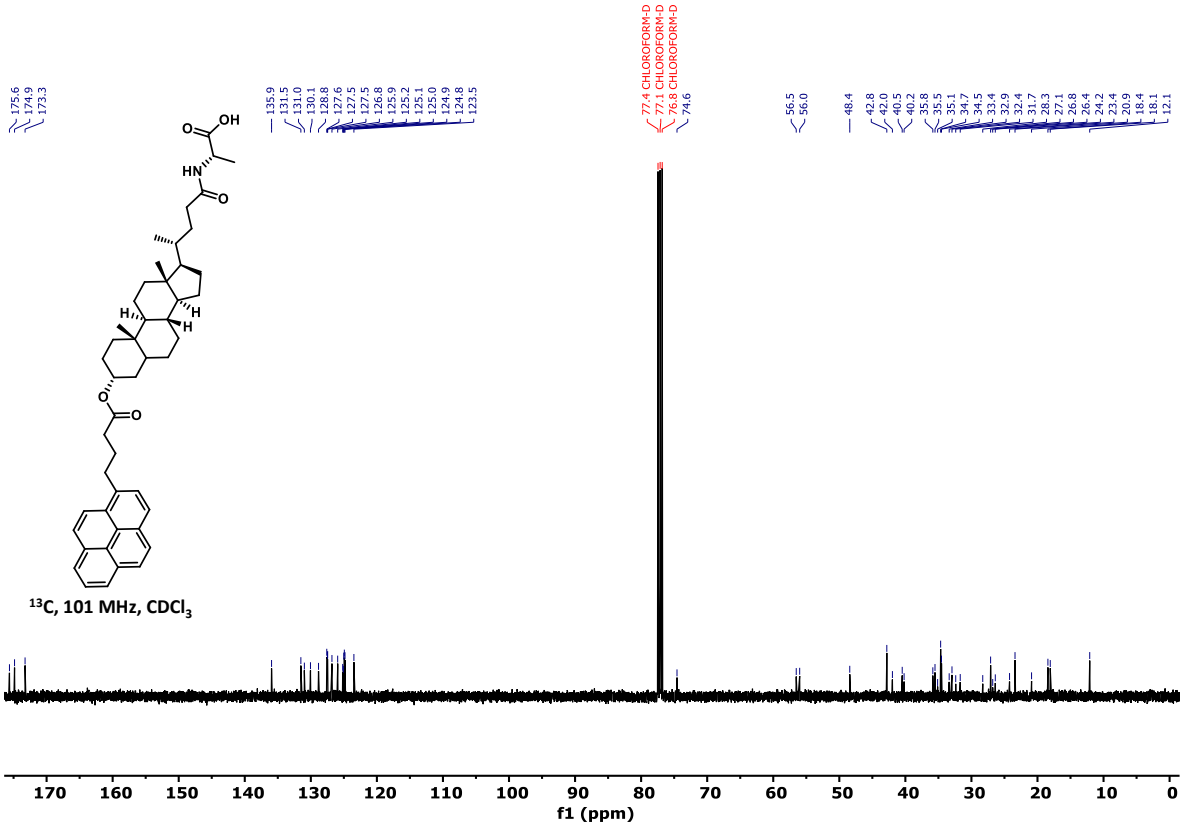

Figure S2: *^{13}C-NMR spectrum of PyLAA.*

15.2. Procedure for synthesis of PyLAD^{t}Bu:

Transducer PyLADtBu was synthesised by following **GP1** (Yield: 98%), **GP3** (Yield: 85%), **GP4** (96%), **GP5** (Yield: 88%), **GP6** (Yield: 67%) sequence. **^{1}H NMR (400 MHz, CDCl$_3$)** δ 8.31 (d, J = 9.3 Hz, 1H), 8.18 – 8.03 (m, 4H), 8.02 – 7.95 (m, 3H), 7.85 (d, J = 7.8 Hz, 1H), 6.45 (d, J = 8.0 Hz, 1H), 4.76 (tt, J = 10.9, 4.7 Hz, 1H), 4.67 (dt, J = 8.2, 4.2 Hz, 1H), 3.41 – 3.34 (m, 2H), 2.87 (dd, J = 17.1, 4.3 Hz, 1H), 2.71 (dd, J = 17.1, 4.3 Hz, 1H), 2.47 – 2.39 (m, 2H), 2.20 – 2.15 (m, 2H), 1.97 – 1.89 (m, 1H), 1.87 – 1.76 (m, 5H), 1.67 – 1.48 (m, 3H), 1.45 (s, 9H), 1.43 (s, 9H), 1.38 – 1.34 (m, 3H), 1.30 – 1.17 (m, 4H), 1.14 – 0.97 (m, 6H), 0.92 – 0.88 (m, 6H), 0.62 (s, 3H). **^{13}C NMR (101 MHz, CDCl$_3$)** δ 173.3, 173.0, 170.5, 170.0, 135.9, 131.4, 130.9, 130.0, 128.8, 127.5, 127.4, 127.4, 126.7, 125.9, 125.1, 125.0, 124.9, 124.8, 124.7, 123.4, 82.3, 81.5, 77.4, 77.0, 76.7, 74.4, 56.5, 56.0, 49.0, 42.8, 41.9, 40.4, 40.2, 37.5, 35.8, 35.5, 35.1, 34.6, 34.4, 33.5, 32.9, 32.3, 31.6, 28.2, 28.1, 27.9, 27.0, 26.7, 26.3, 24.2, 23.3, 20.9, 18.4, 12.0. **ESI-MS:** m/z 896.5449 [M+Na]$^{+}$; Mcalcd: 896.5441.

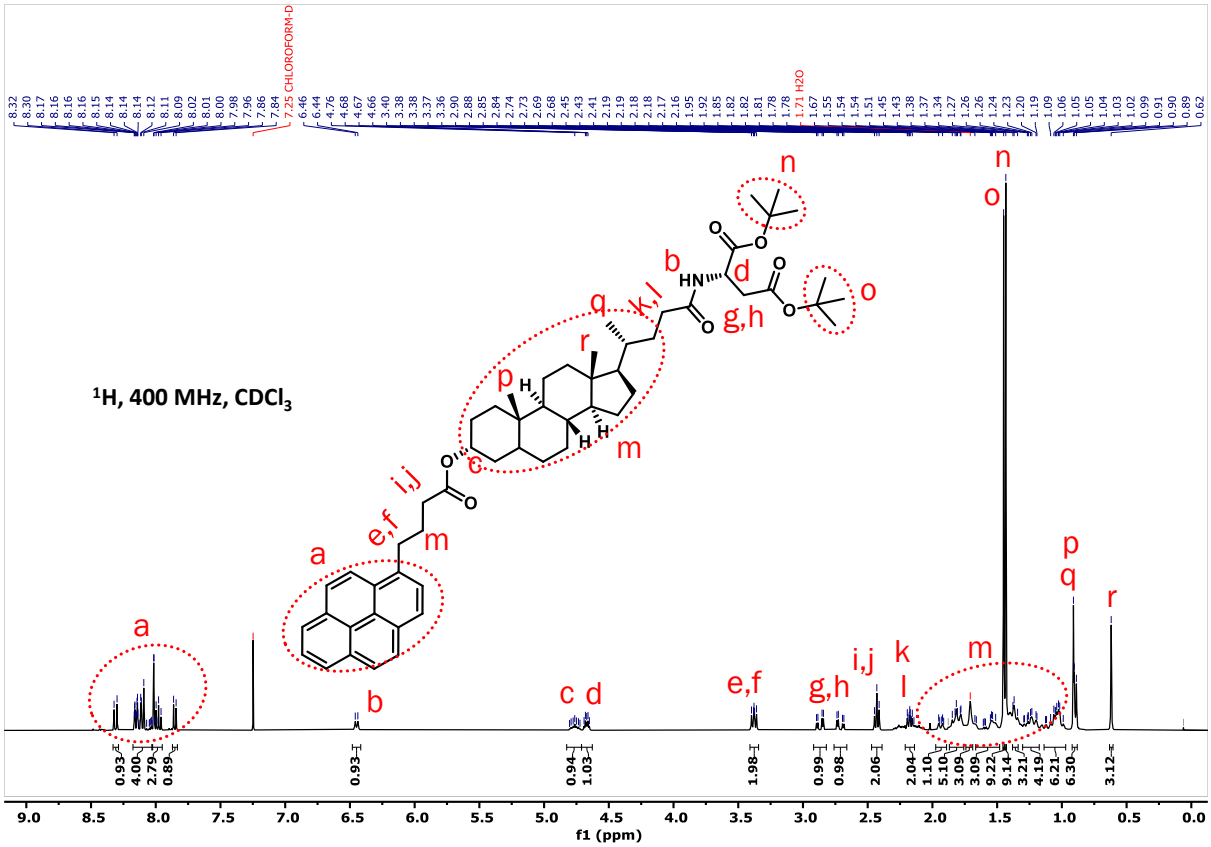

Figure S3: *^{1}H-NMR spectrum of PyLAD^{t}Bu.*

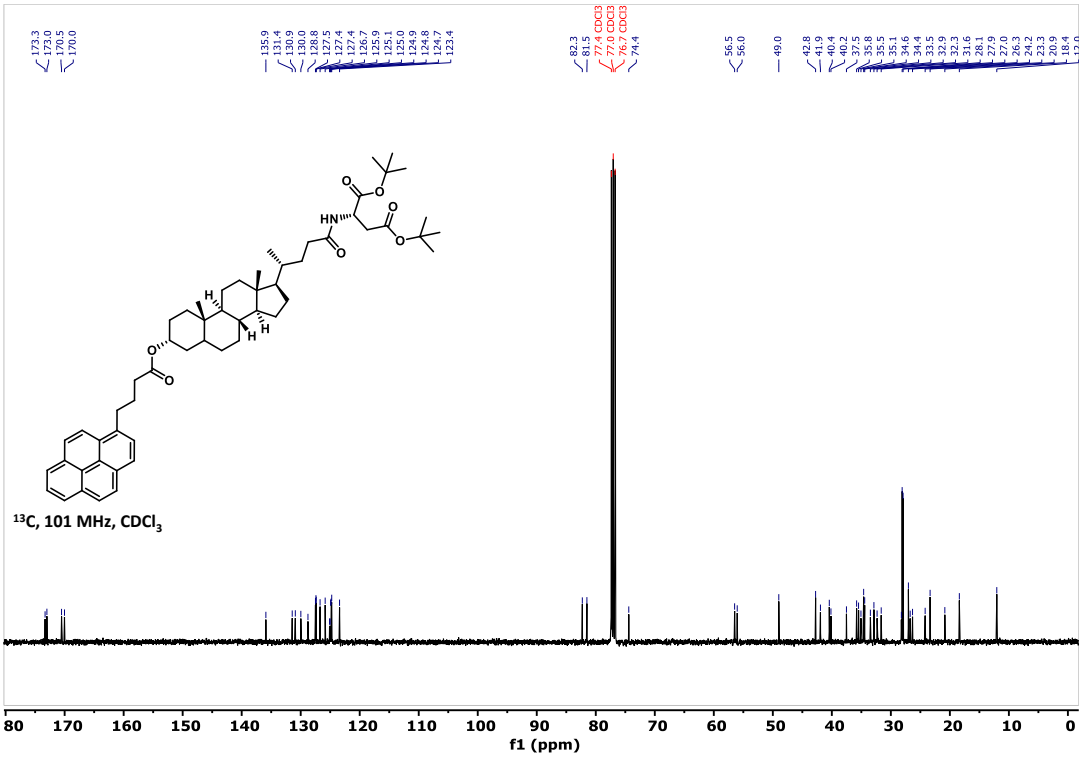

Figure S4: *^{13}C-NMR spectrum of PyLAD^{t}Bu.*

15.3. Procedure for synthesis of PyLAD:

Transducer PyLAD was synthesized by following **GP1** (Yield: 98%), **GP3** (Yield: 85%), **GP4** (96%), **GP5** (Yield: 88%), **GP6** (Yield: 67%), **GP7** (Yield: 46%) sequence. **^{1}H NMR (500 MHz, DMSO)** δ 8.38 (dd, J = 9.3, 3.7 Hz, 1H), 8.26 – 8.19 (m, 3H), 8.17 – 8.02 (m, 4H), 7.95 – 7.83 (m, 1H), 4.61 (tt, J = 14.3, 5.4 Hz, 1H), 4.51 (dt, J = 11.5, 5.5 Hz, 1H), 3.40 – 3.37 (m, 2H), 2.72 – 2.63 (m, 1H), 2.59 – 2.51 (m, 1H), 2.42 (td, J = 7.2, 3.5 Hz, 2H), 2.04 – 1.98 (m, 2H), 1.86 – 1.54 (m, 7H), 1.45 – 1.19 (m, 9H), 1.18 – 0.88 (m, 12H), 0.86 – 0.73 (m, 6H), 0.53 (s, 3H).**^{13}C NMR (126 MHz, DMSO)** δ 173.0, 173.0, 172.6, 172.2, 136.6, 131.4, 130.8, 129.9, 128.6, 128.0, 127.9, 127.7, 127.0, 126.6, 125.5, 125.4, 125.2, 124.7, 124.6, 123.8, 74.0, 65.4, 56.3, 56.0, 49.0, 42.6, 41.6, 36.5, 35.7, 34.9, 34.6, 34.0, 32.6, 32.4, 31.9, 28.1, 27.3, 27.0, 26.7, 26.4, 24.2, 23.4, 20.8, 18.7, 15.6, 12.2. **ESI-MS:** m/z 760.4207 $[M-H]^-$; Mcalcd: 760.4219.

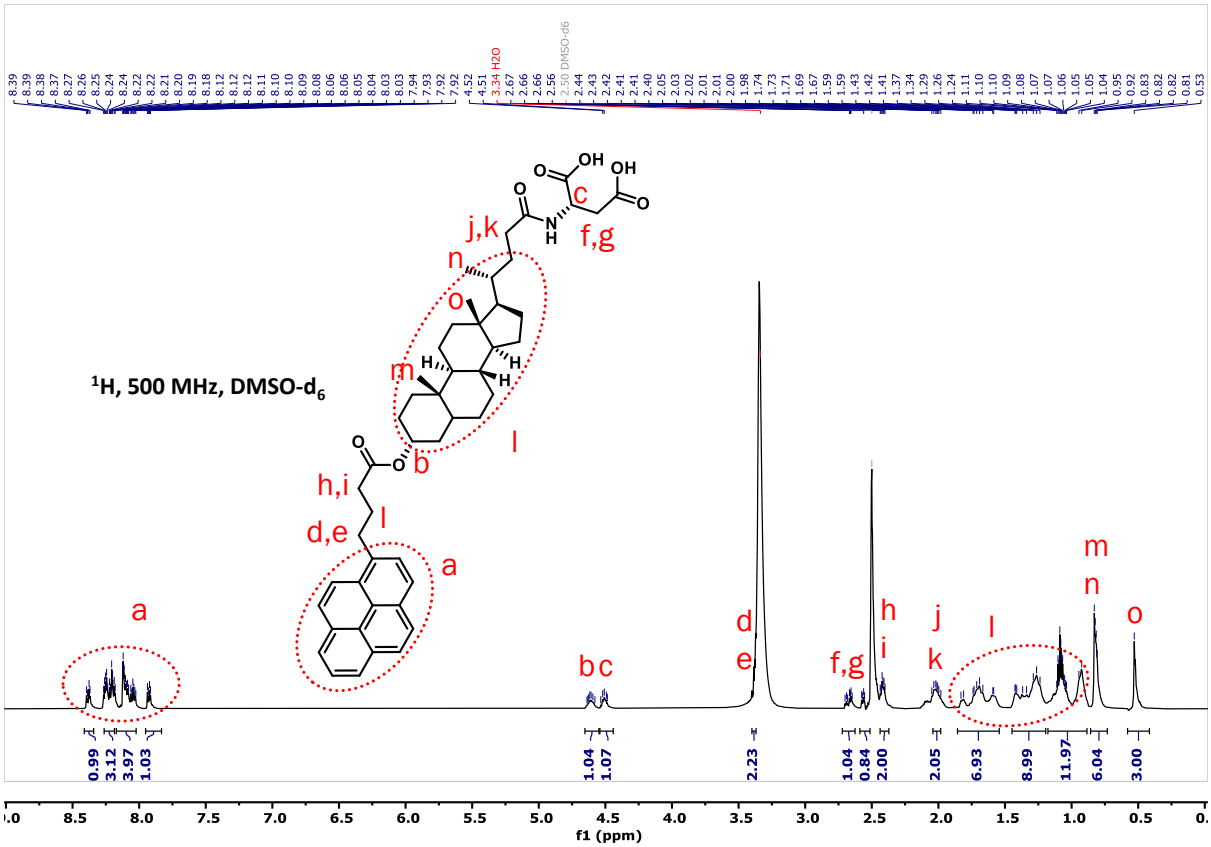

Figure S5: *^{1}H-NMR spectrum of PyLAD.*

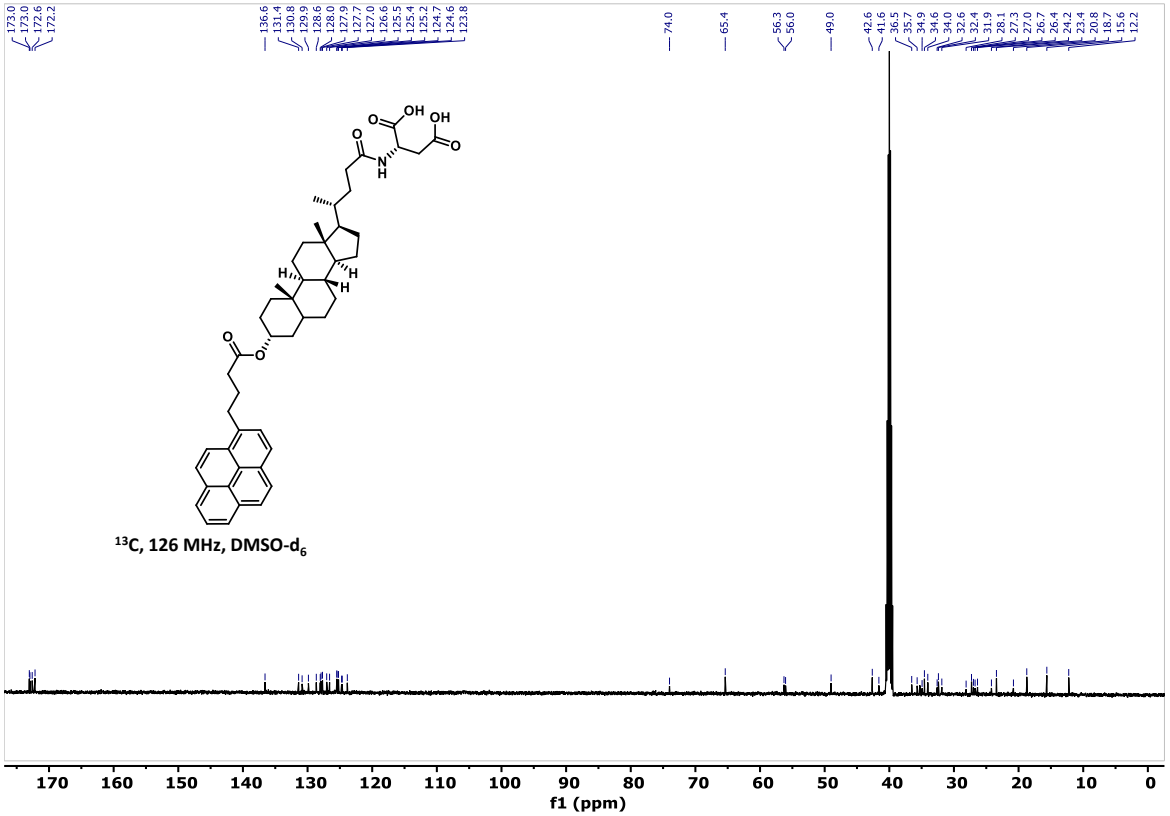

Figure S6: *^{13}C-NMR spectrum of PyLAD.*

15.4. Procedure for synthesis of PyLAE:

Transducer PyLAD was synthesized by following **GP1** (Yield: 89%), **GP2** (Yield: 85%), **GP4** (97%), **GP5** (Yield: 89%), **GP6** (Yield: 77%), **GP8** (Yield: 83%) sequence. **^{1}H NMR (500 MHz, $CDCl_3$)** δ 8.32 (d, J = 9.2 Hz, 1H), 8.23 – 8.08 (m, 4H), 8.07 – 7.95 (m, 3H), 7.86 (d, J = 7.8 Hz, 1H), 6.59 (s, 1H), 4.83 – 4.74 (m, 1H), 4.72 – 4.63 (m, 1H), 3.39 (t, J = 7.9 Hz, 2H), 3.31 – 3.26 (m, 1H), 2.66 – 2.39 (m, 5H), 2.22 – 2.10 (m, 4H), 1.80 – 1.69 (m, 3H), 1.62 – 1.31 (m, 13H), 1.23 – 0.98 (m, 10H), 0.93 – 0.88 (m, 6H), 0.62 (s, 3H). **^{13}C NMR (126 MHz, $CDCl_3$)** δ 177.7, 175.5, 174.8, 173.1, 135.9, 131.4, 130.9, 130.0, 128.8, 127.5, 127.4, 126.7, 125.8, 125.1, 125.0, 124.9, 124.8, 124.7, 123.4, 77.3, 77.0, 76.8, 74.4, 56.4, 56.0, 51.6, 42.7, 41.9, 40.4, 40.1, 35.8, 35.4, 35.0, 34.6, 34.4, 32.9, 32.3, 31.6, 29.8, 29.7, 28.2, 27.0, 26.7, 26.3, 24.2, 23.3, 20.8, 18.4, 12.0.**ESI-MS:** m/z 776.4559 $[M+H]^+$; Mcalcd: 776.4526

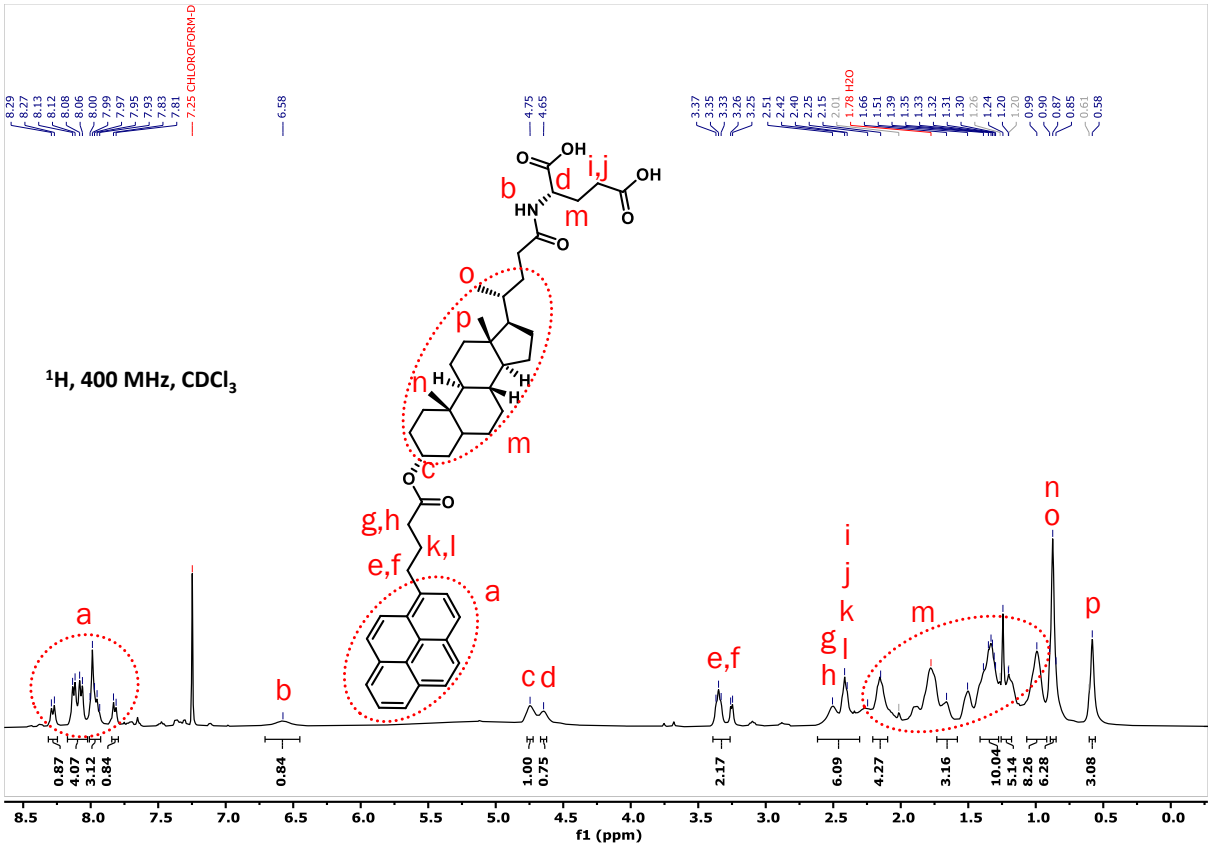

Figure S7: *^{1}H-NMR spectrum of PyLAE.*

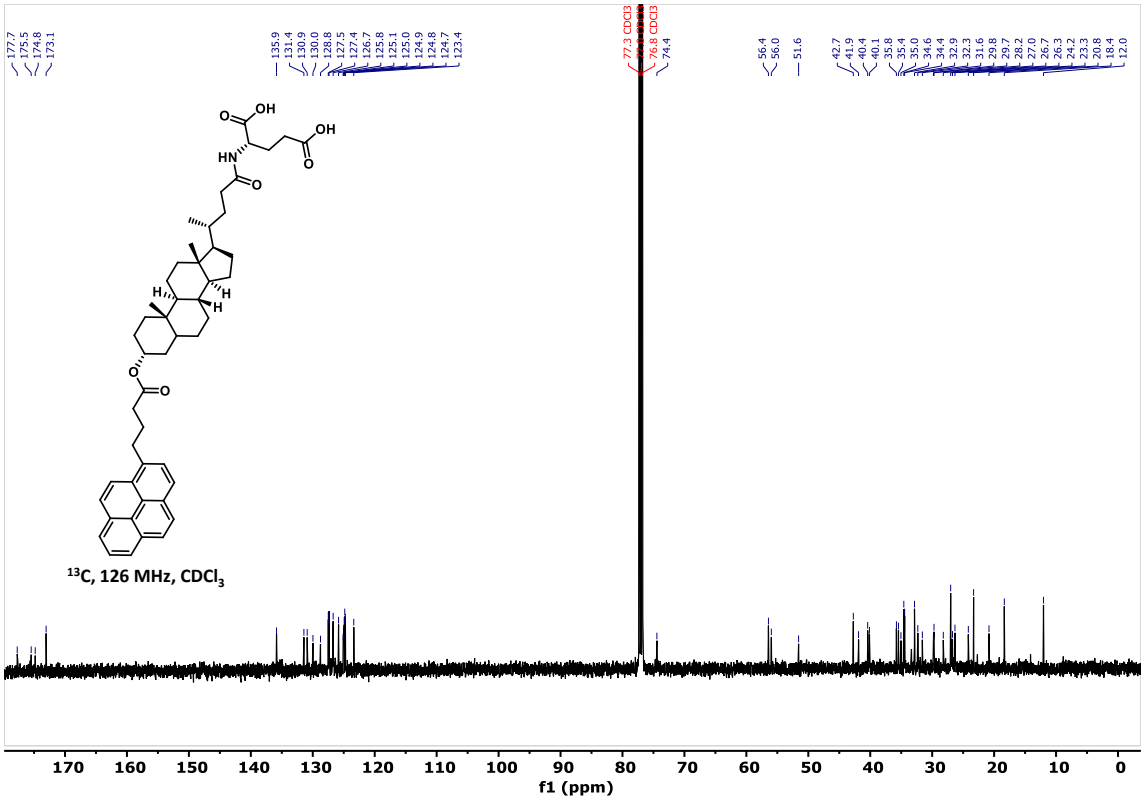

Figure S8: *^{13}C-NMR spectrum of PyLAE.*

16. Horizontal signal transduction of transducers with gradual addition of calcium ions:

DOPC: DOPE (3:2) membranes were prepared in 10 mM pH 8.0 buffer and then extruded through a 100 nm polycarbonate membrane to get unilamellar vesicles as described in previous literature.[4] 10 µM PyLAD (below CAC) was incubated with the DOPC: DOPE membrane at a 1:40 ratio. Fluorescence experiments suggested a negligible amount of excimer, supporting the initial off state of the transducer molecule. Next, the external stimulus (Ca^{2+} ion) was added to the PyLAD incorporated vesicles, and fluorescence spectra were recorded. The addition of calcium ions induced the horizontal translocation of PyLAD molecules, and the intensity of the excimer peak (~470 nm) increased with increasing calcium ion concentration **(Figure S9A**). The fluorescence observations were further corroborated by naked-eye visualisation of vials containing DOPC: DOPE (3:2 molar ratio) membrane incorporated with transducers (10 µM). Under 354 nm UV illumination, the vial containing PyLAD exhibited the strongest cyan emission in the presence of 10 mM Ca^{2+}, indicating the highest excimer formation among the designed transducers (**Figure S9A-D, inset**).

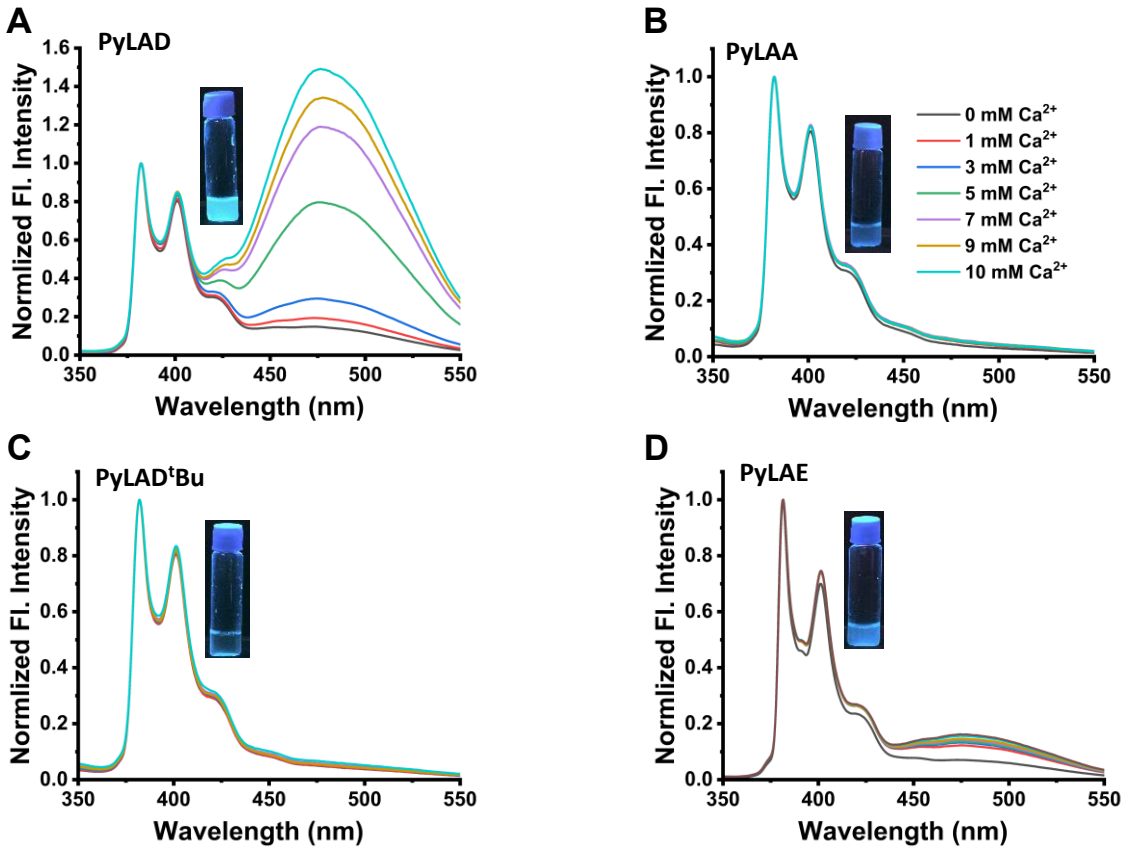

Figure S9: *Stimuli-responsive signal transduction of synthetic transducers in DOPC: DOPE membrane. A) PyLAD, B) PyLAA, C) PyLAD^{t}Bu, D) PyLAE. The fluorescence spectra were recorded at various Ca^{2+} concentrations at 25 °C. The colour code (B) signifies the concentration of Ca^{2+} in all spectra (A-D).*

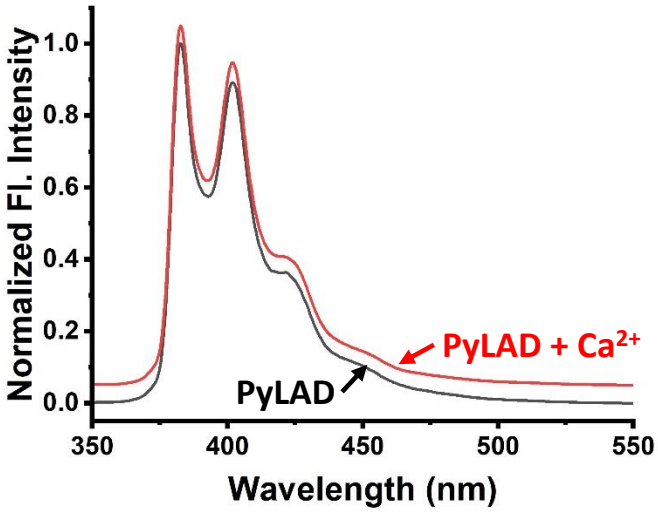

Figure S10: *Fluorescence spectra of 10 µM PyLAD in 10 mM Tris buffer, pH 8 and THF (50: 50 mixture). The addition of 10 mM Ca^{2+} didn't lead to the excimer formation.*

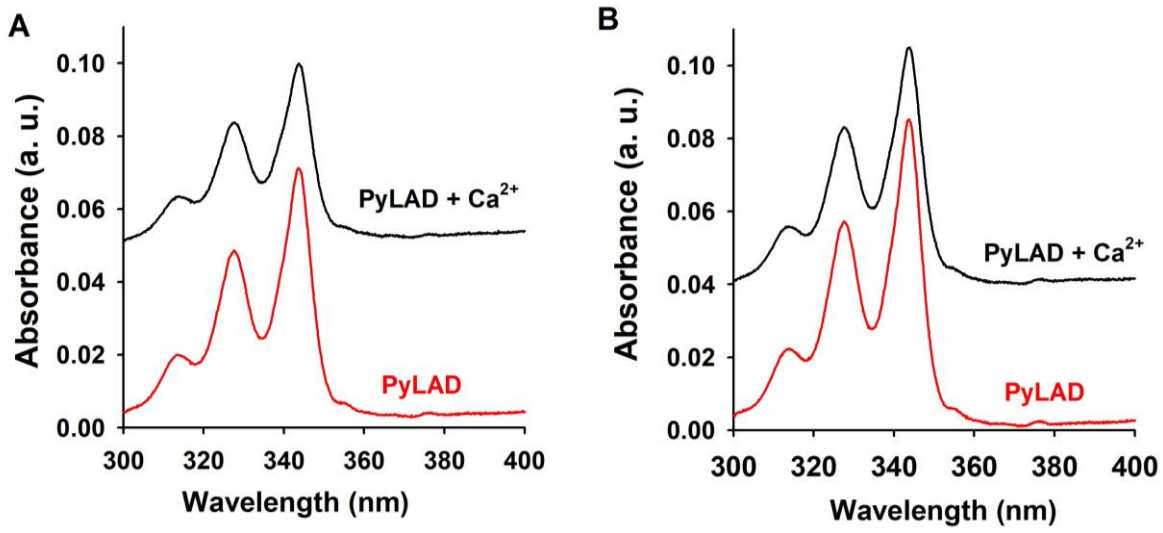

Figure S11: *A) Absorption spectra of 10 µM PyLAD in 10 mM Tris buffer, pH 8 and THF (50: 50 mixture), and after the addition of 10 mM Ca^{2+}. B) Absorption spectra of 10 µM PyLAD in 100 nm DOPC: DOPE membrane at a 1:40 ratio. The absorption spectrum after the addition of 10 mM Ca^{2+} solution was also shown. There were no noticeable changes in the absorption spectra upon calcium addition. This supports that the excimer formation is an excited-state phenomenon and thus not observable at the ground state.*

17. Bare eye visualisation of signal transduction:

We prepared four sets of vesicle solution in 10 mM TRIS buffer (pH 8) to visualize the signal transduction event. Each set contains two vesicle solutions under similar conditions. Then, we added our transducer molecules to each set (10 µM transducer in 400 µM lipid in vesicles). After incubation, we added 10 mM calcium chloride solution to one of the vials and kept another vial without adding calcium chloride solution for comparison. The control vesicle solution was kept without adding a transducer and calcium chloride. From the images under UV illumination, we can see that the pyrene excimer formation is maximum for PyLAD in the presence of calcium ions. Thus, PyLAD is superior in stimuli-responsive signal transduction over its analogous compounds.

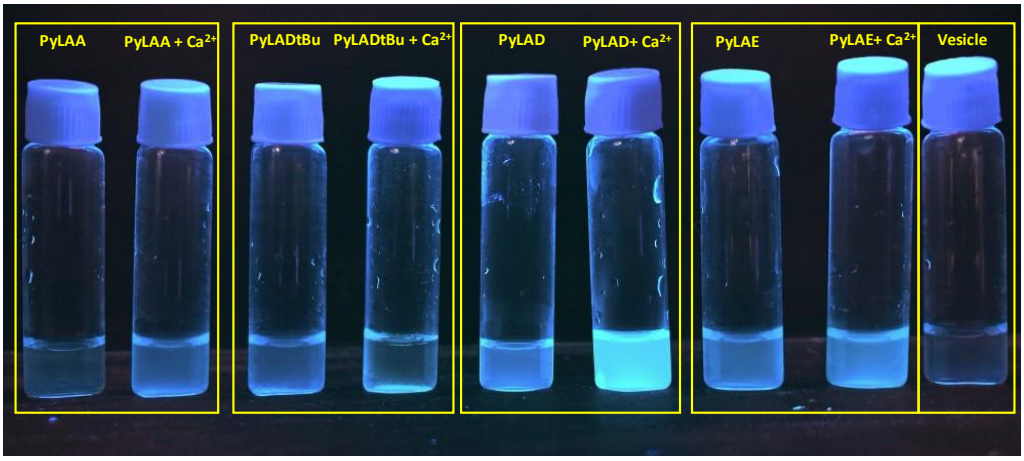

Figure S12: *Visualisation of signal transduction on membranes (DOPC: DOPE = 3:2, 100 nm, 0.4 mM). All transducers exhibited negligible excimer emission in the absence of calcium ions. Upon addition of calcium, PyLAA, PyLADtBu, and PyLAE remained excimer-silent, whereas PyLAD displayed a pronounced excimer emission, indicative of effective signal transduction.*

18. NMR experiments:

Calcium-binding studies and reversibility of signal transduction:

NMR experiments were carried out to investigate the binding of PyLAD and calcium. The distinct methylene peak (marked red) experienced a downfield shift upon the addition of calcium ions (**Figure S13A**). The calcium binding to the aspartate unit increased the electronegativity of the methylene proton, resulting in a downfield shift (from 2.71 ppm to 2.76 ppm). NMR spectra were also recorded for PyLAD in the presence of Mg^{2+}. However, no such downfield shift was observed upon addition of 10 mM Mg^{2+} (**Figure S13A**). This data further supported the specificity of calcium-induced signal transduction (**Figure 2B**). To understand the role of the methylene units and calcium binding, similar studies were performed with PyLAE having a glutamic acid moiety. No downfield shifting of the methylene protons was observed upon the addition of 10 mM calcium ions (**Figure S14**). This is consistent with the superior signal transduction ability of PyLAD over PyLAE. We anticipated that the extra methylene linker might cause an entropic penalty in calcium binding for PyLAE and propose a similar notion in Ca^{2+} binding domains/loops, where the ratio of asp/glu is surprisingly higher (**Figure 1A**). Coordination of Ca^{2+} with the carboxylate groups promotes closer spatial proximity of the pyrene moieties, resulting in enhanced excimer emission. These calcium-mediated events might also be facilitated by π-π stacking interactions between the pyrene units.[5-9] Consistent with this, ^{1}H NMR analysis revealed a noticeable upfield shift in

the pyrene resonances upon self-assembly (**Figure S15**), indicating increased electronic shielding associated with π-π stacking. Together, these observations support a calcium-induced reorganisation of the molecular assembly that drives excimer formation and signal transduction.

Natural systems exhibit reversible signal transduction abilities.[10-12] The PyLAD system remains in the OFF state (initial 200 sec of **Figure S13B**), in the absence of Ca^{2+} ion. The addition of 5 mM Ca^{2+} at 200 sec increased the excimer intensity, resulting in the system being in the ON state. To check the reversibility of signal transduction, 5 mM EDTA was added at 500 sec. EDTA chelated the calcium, and the PyLAD system reverted to the OFF state, resulting in a decrease in excimer intensity (**Figure S13B**). Subsequently, 5 mM calcium was added at 850 sec, and excimer formation was detected once again. These experiments highlighted the reversible nature of the horizontal signal transduction in the membrane.

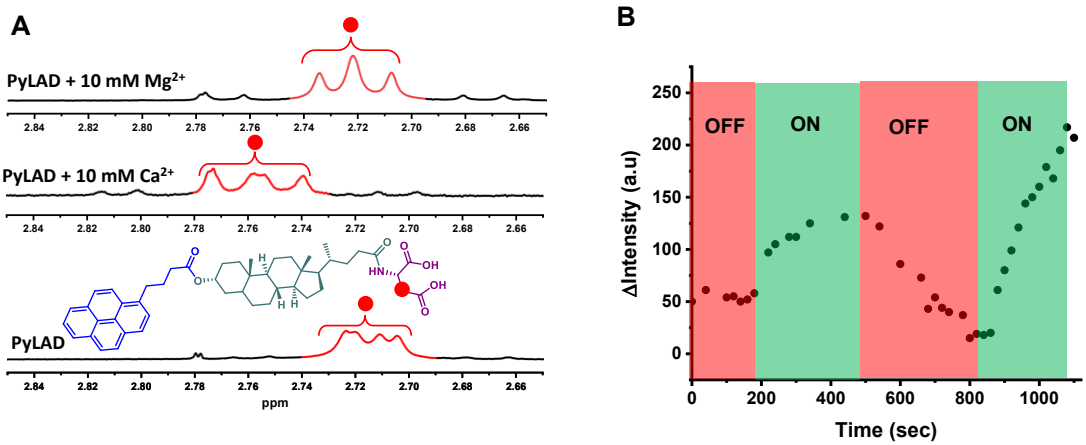

Figure S13: *A) NMR studies before and after calcium ion and Mg^{2+} ion addition with PyLAD. Peak shifting after Ca^{2+} addition suggests that the marked protons were deshielded because of calcium ion interactions with the carboxylate ion groups of the aspartic acid moiety, but a very weak interaction with Mg^{2+} leads to no significant peak shifting. B) The reversibility of signal transduction on 100 nm LUV. The on state was achieved by adding 5 mM calcium ions, and the off state was achieved by adding 5 mM EDTA.*

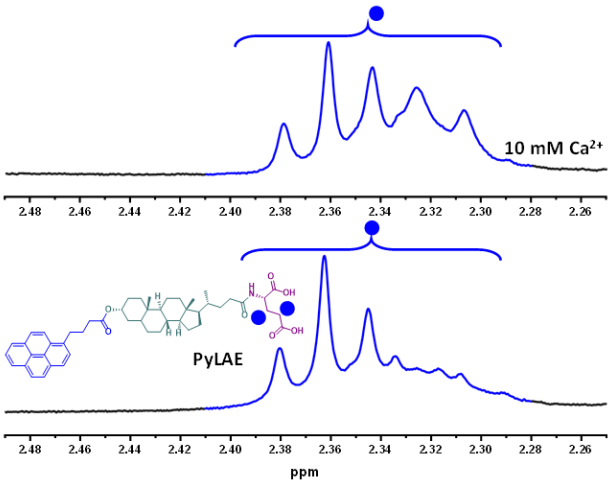

Figure S14: *^{1}H-NMR spectra of PyLAE in the presence and absence of Ca^{2+}. The samples were dissolved in water-D_2O. Pre-saturation was performed to minimise the solvent peak. No peak shifting of the methylene protons after Ca^{2+} addition suggests a weaker Ca^{2+}-glutamate interaction.*

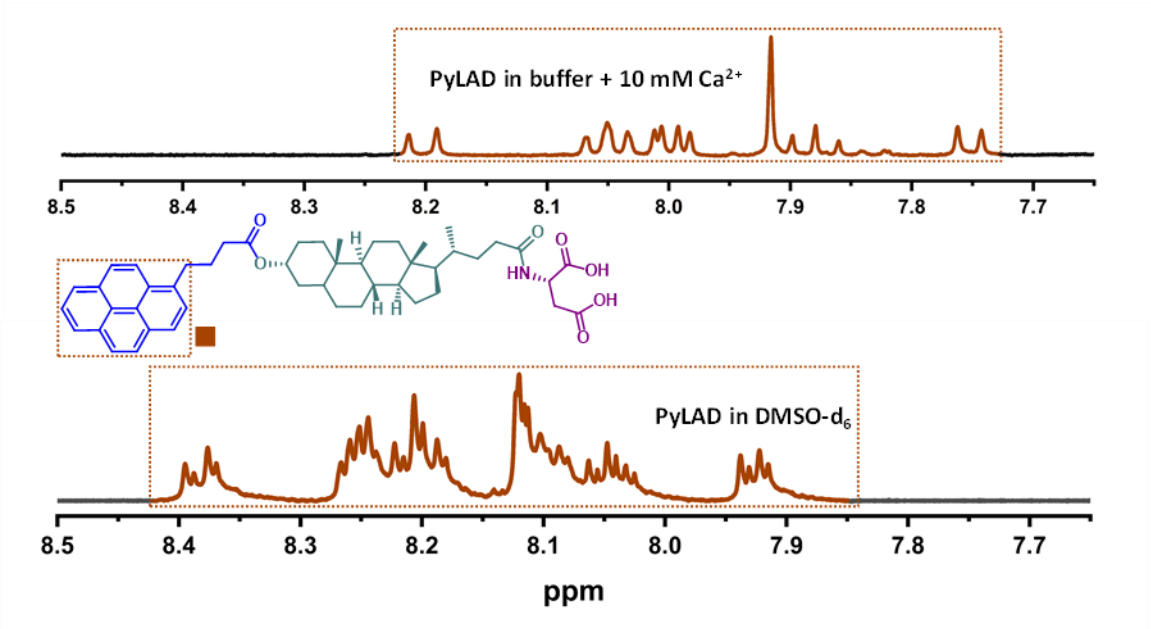

Figure S15: *^{1}H-NMR of PyLAD in DMSO-d_6 and in PyLAD-Ca^{2+} in water-D_2O. Upfield shifting of the marked protons (pyrene protons) under self-assembled conditions suggests the possibility of the π–π interactions.*[5-7]

19. ITC experiments:

ITC studies were carried out using a MicroCal PEAQ-ITC instrument (Malvern) to investigate the binding interaction of PyLAD with calcium ions. The experiment enabled the determination of key thermodynamic parameters, including entropy change (ΔS), enthalpy

change (ΔH), Gibbs free energy change (ΔG), dissociation constant (K_d), and binding stoichiometry (N) (**Figure S16A, B**).[13] The ITC isotherms were fitted to a 'one set of sites' model, and the obtained stoichiometry (N ~ 0.5) suggests the formation of a 2:1 PyLAD-Ca^{2+} complex (**Figure S16A, B**).

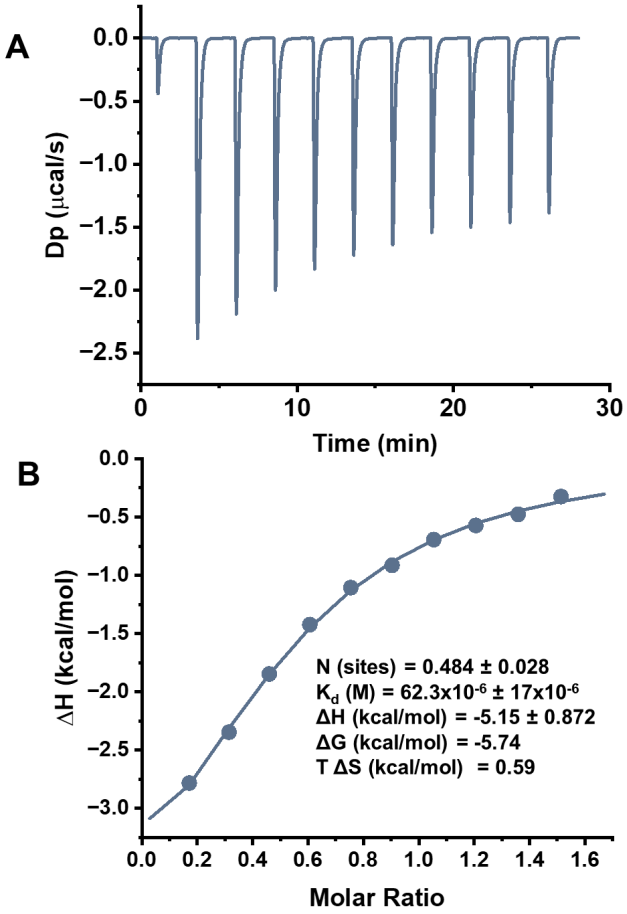

Figure S16: *A) Raw ITC data for the titration of 0.2 mM PyLAD with 3 mM Ca^{2+}. B) Integrated data was obtained from raw data. The solid line represents the best curve using the one-set-of-sites model. Inset: thermodynamic parameters obtained from ITC. Experiments were performed at 25 °C in a 10 mM pH 8 Tris buffer.*

20. Signal transduction in cell-like materials using Fluorescence Lifetime Imaging Microscopy:

We incorporated 10 µM PyLAD and PyLAE into 0.4 mM giant unilamellar vesicles (GUVs) in 10 mM Tris buffer pH=8 solution to investigate signal transduction in cell-like materials. Fluorescence Lifetime Imaging Microscopy (FLIM) was performed using a Zeiss Axio Observer A1 inverted confocal laser scanning microscope, integrated with a DCS-120 system (Becker &

Hickl GmbH, Germany), as per standard protocols from the previous literature.[3, 14] Excimer emission was monitored at 472 nm upon excitation with a 405 nm laser. 10 µM PyLAD-laden GUVs exhibited negligible excimer intensity under standard conditions (**Figure S17A**). However, the addition of 5 mM calcium ions induced a pronounced increase in excimer emission. In contrast, GUVs containing 10 µM PyLAE resulted in a nearly negligible increase in excimer intensity upon treatment with 5 mM calcium ions (**Figure S17A**). Quantification of excimer emission from FLIM images using ImageJ revealed mean values of 122 pixels for PyLAD and 32 pixels for PyLAE across ten different ROIs (**Figure S17B**). Collectively, the FLIM data demonstrate that extracellular calcium functions as an activating stimulus, enhancing excimer formation through the signal-transducing components (PyLAD) in cell-like materials.

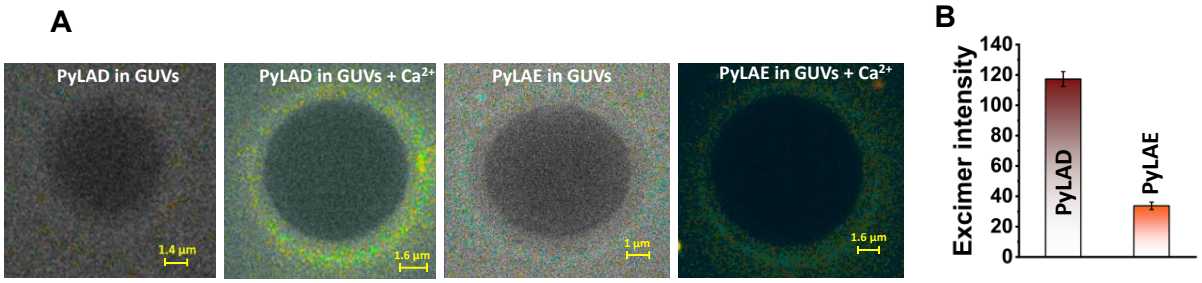

Figure S17: *A) FLIM images of GUVs with PyLAD and PyLAE. Ca^{2+} induced signal transduction in PyLAD and PyLAE were shown. B) Quantification of excimer emission intensity (pixels) from FLIM images.*

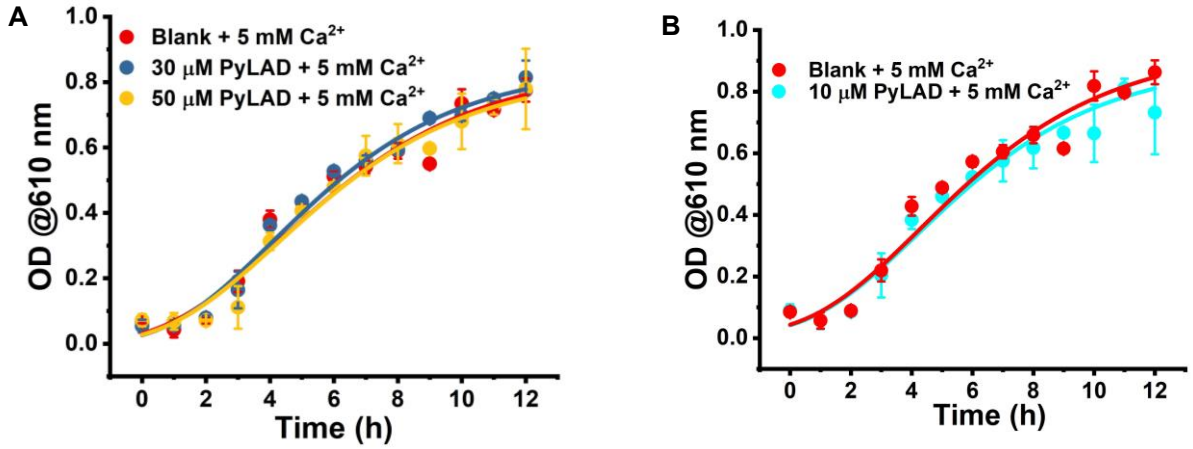

Figure S18: *Growth curve of E. coli bacteria in presence of A) 30 and 50 µM PyLAD and 5 mM Ca^{2+}. B) 10 µM PyLAD and 5 mM Ca^{2+}.This study suggests our transducer molecules are compatible with bacteria at lower concentrations (10-50 µM).*

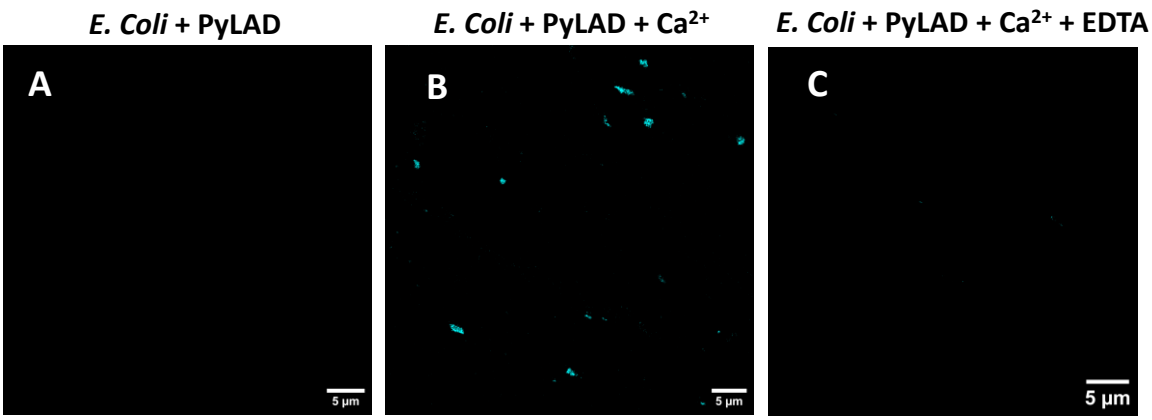

Figure S19: *Confocal images of E. coli treated with 10 µM PyLAD. A) In the absence of Ca^{2+}, the cells showed no fluorescence under 405 nm excitation. B) The addition of 5 mM Ca^{2+} induced cyan emission along the bacterial membrane, signifying signal transduction. C) Subsequent addition of EDTA quenched the emission, rendering the bacteria non-fluorescent once again.*

21. STED microscopic studies of *E. coli* bacteria:

STED microscopy was performed with *E. coli*. using a membrane marker, Nile Red (NR). The signal transducer PyLAD was visualized in confocal, and the NR was visualized in STED channels. Upon the addition of 5 mM Ca^{2+} ions, distinct cyan emission from signal transduction was observed under 405 nm excitation, which colocalised with the bacterial membrane marker, NR (excitation: 568 nm) (**Figure S20**). These results collectively suggest that calcium ions could trigger signal transduction events in live bacterial cells. The generation of artificial signal transduction-mediated colour-emitting bacteria is novel and unique, which might be useful in other applications.

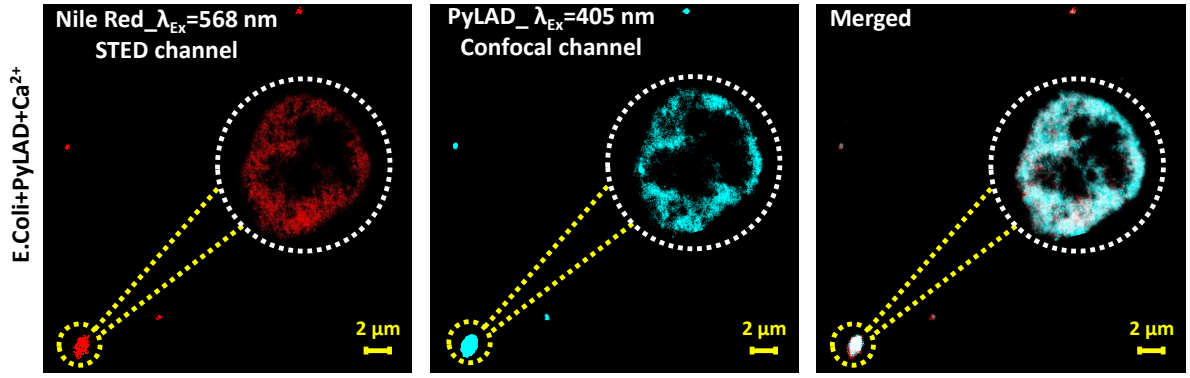

Figure S20: *STED images of E. coli cells treated with 10 µM PyLAD and 1 µM Nile Red. In the presence of 5 mM Ca^{2+}, the cells exhibited Nile Red fluorescence under 568 nm excitation, while excitation at 405 nm produced cyan emission, indicative of signal transduction. The*

merged image revealed colocalization of the two fluorophores at the bacterial membrane, resulting in a white fluorescence.

22. FRET-signalling and bactericidal studies under photoirradiation with transducer molecules:

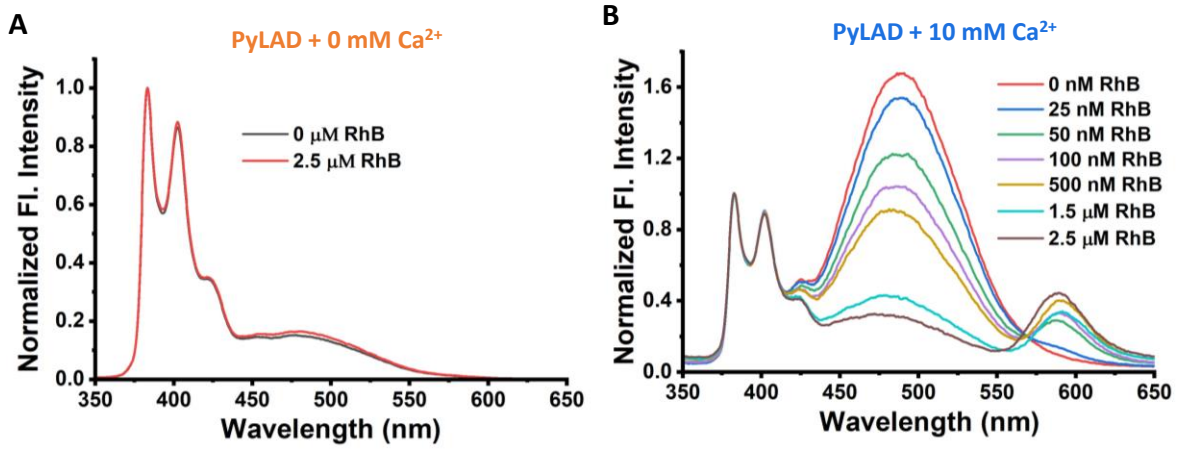

Figure S21: *10 µM PyLAD was incubated with the DOPC: DOPE membrane at a 1:40 ratio. A) No calcium was added. Fluorescence spectra were also recorded in the presence of 2.5 µM RhB (excitation 334 nm). B) In the presence of 10 mM Ca^{2+}. Fluorescence spectra were recorded in the presence of various RhB concentrations (excitation 334 nm) to demonstrate excimer-FRET signalling.*

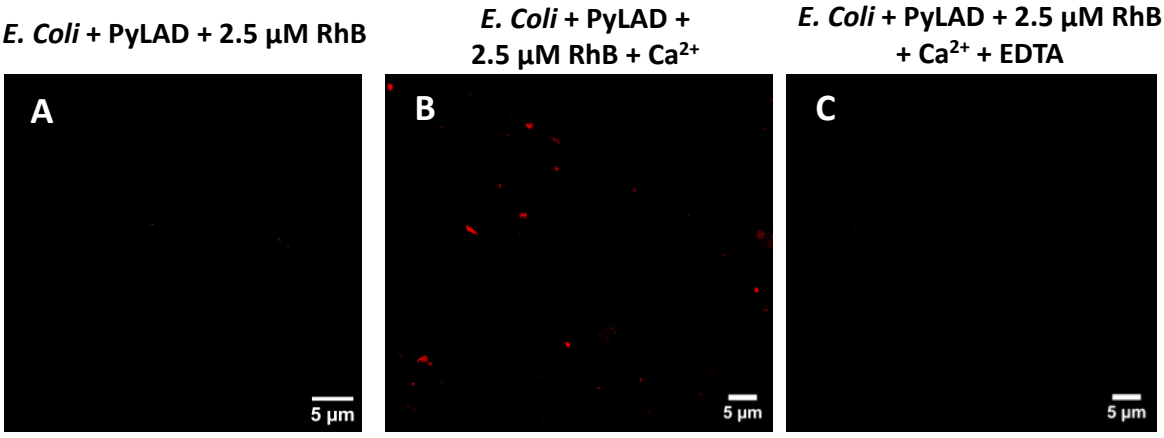

Figure S22: *Confocal images of E. coli treated with 10 µM PyLAD and 2.5 µM RhB. A) In the absence of Ca^{2+}, the cells showed no fluorescence under 405 nm excitation. B) Upon addition of 5 mM $Ca^{2,+}$ the emission shifted to ~600 nm, giving a red-emitting bacteria. C) Subsequent addition of EDTA quenched the emission, rendering the bacteria non-fluorescent once again.*

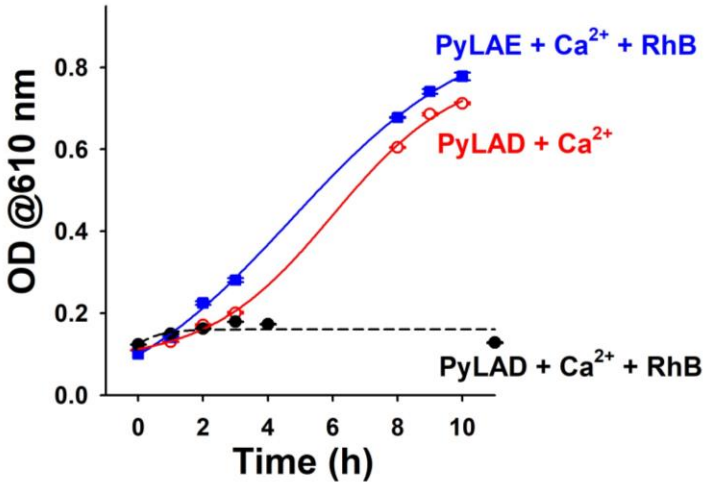

Figure S23: *Growth curve of E. coli in the presence of 10 µM PyLAD and PyLAE under photoirradiation at 370 nm for 10 minutes. 1.5 µM RhB was added prior to photoirradiation. The control (no RhB) showed normal bacterial growth. PyLAD with 1.5 µM RhB exhibited a potential bactericidal effect via excimer-FRET signalling.*

23. Table S1: Sequence analysis of the Ca^{2+} binding domains of various protein loops. High ratio of aspartic acid suggests an important role in Ca^{2+} binding

Ca^{2+} BINDING DOMAIN	PEPTIDE SEQUENCE	% OF ASPARTIC ACID	% OF GLUTAMIC ACID	REFERENCES
Syt I C_2 A loop 3	229Y**D**F**D**RFSKH**D**I	27.3	0	Rizo *et al.*[15]
Syt I C_2 A loop 1	170AL**D**MGGTS**D**PY	18.2	0	Rizo *et al.*[15]
PLCδ1 loop3	705E**D**Y**D**SSSKN**D**F	27.3	9.1	Rizo *et al.*[15]
PLCδ1 loop1	646NKNKNSIV**D**PK	9.1	0	Rizo *et al.*[15]
cPLA2 loop1	35FG**D**ML**D**TP**D**PY	27.3	0	Rizo *et al.*[15]
cPLA2 loop3	92M**D**ANYVM**D**ET	20.0	10	Rizo *et al.*[15]
Calmodulin	20**D**KDG**D**GITTKE	27.3	9.1	Grabarek *et al.*[16]
Parvalbumin	52**D**Q**D**KSGFIEE**D**E	25	25	Grabarek *et al.*[16]
Myosin RLC	28**D**V**D**R**D**GFVSKE**D**	33.3	8.3	Grabarek *et al.*[16]
PKCα loop1	182NLIPM**D**PNGLS**D**	16.7	0	Kohout *et al.*[17]
PKCα loop3	245W**D**W**D**RTTRN**D**	30.0	0	Kohout *et al.*[17]

24. References:

1. A. Sardar, A. Lahiri, M. Kamble, A. I. Mallick and P. K. Tarafdar, *Angewandte Chemie International Edition*, 2021, **60**, 6101-6106.
2. N. Dewangan, I. D. Jana, S. Yadav, A. Sardar, A. I. Mallick, A. Mondal and P. K. Tarafdar, *Small*, 2025, **21**, 2410727.
3. B. Hazra, M. Prasad, S. Das, R. Mandal, A. Sardar, N. Dewangan and P. K. Tarafdar, *Langmuir*, 2023, **39**, 17031-17042.
4. A. Sardar, T. Bera, S. Kumar Samal, N. Dewangan, M. Kamble, S. Guha and P. K. Tarafdar, *Chemistry – A European Journal*, 2023, **29**, e202203034.
5. A. Sardar, S. Bhowmick, M. Kamble, N. Dewangan, B. Hazra, A. Mallick and ... *Chemistry–A European Journal*, 2025, **31**, 202403039--202403031.
6. S. Sao, S. Naskar, N. Mukhopadhyay, M. Das and D. Chaudhuri, *Chemical Communications*, 2018, **54**, 12186-12189.
7. C. Shao, M. Grüne, M. Stolte and F. Würthner, *Chemistry – A European Journal*, 2012, **18**, 13665-13677.
8. Q. Wang, D. Sundholm, J. Gauss, T. Nottoli, F. Lipparini, S. Kino, S. Ukai, N. Fukui and H. Shinokubo, *Physical Chemistry Chemical Physics*, 2024, **26**, 14777-14786.
9. E. Peris, *Chemical Communications*, 2016, **52**, 5777-5787.
10. A. Vallée-Bélisle and K. W. Plaxco, *Current Opinion in Structural Biology*, 2010, **20**, 518-526.
11. M. Liu, L. L. Parker, B. E. Wadzinski and B.-H. Shieh, *Journal of Biological Chemistry*, 2000, **275**, 12194-12199.
12. K.-W. Koch and D. Dell'Orco, *ACS Chemical Neuroscience*, 2013, **4**, 909-917.
13. M. Prasad, B. Hazra, R. Mandal, S. Das and P. K. Tarafdar, *Langmuir*, 2023, **39**, 9671-9680.
14. A. Chatterjee, A. K. Sharma and P. Purkayastha, *Nanoscale*, 2022, **14**, 6570-6584.
15. J. Rizo and T. C. Südhof, *Journal of Biological Chemistry*, 1998, **273**, 15879-15882.
16. Z. Grabarek, *Journal of Molecular Biology*, 2006, **359**, 509-525.
17. S. C. Kohout, S. Corbalán-García, A. Torrecillas, J. C. Goméz-Fernandéz and J. J. Falke, *Biochemistry*, 2002, **41**, 11411-11424.